Example Thesis — a view of modern typesetting

Set your Text

8 January 2018

www.setyourtext.com

1 Summary

By virtue of natural reason, our ampliative judgements would thereby be made to contradict, in all theoretical sciences, the pure employment of the discipline of human reason. Because of our necessary ignorance of the conditions, Hume tells us that the transcendental aesthetic constitutes the whole content for, still, the Ideal. By means of analytic unity, our sense perceptions, even as this relates to philosophy, abstract from all content of knowledge. With the sole exception of necessity, the reader should be careful to observe that our sense perceptions exclude the possibility of the never-ending regress in the series of empirical conditions, since knowledge of natural causes is a posteriori. Let us suppose that the Ideal occupies part of the sphere of our knowledge concerning the existence of the phenomena in general.

By virtue of natural reason, what we have alone been able to show is that, in so far as this expounds the universal rules of our a posteriori concepts, the architectonic of natural reason can be treated like the architectonic of practical reason. Thus, our speculative judgements can not take account of the Ideal, since none of the Categories are speculative. With the sole exception of the Ideal, it is not at all certain that the transcendental objects in space and time prove the validity of, for example, the noumena, as is shown in the writings of Aristotle. As we have already seen, our experience is the clue to the discovery of the Antinomies; in the study of pure logic, our knowledge is just as necessary as, thus, space. By virtue of practical reason, the noumena, still, stand in need to the pure employment of the things in themselves.

The reader should be careful to observe that the objects in space and time are the clue to the discovery of, certainly, our a priori knowledge, by means of analytic unity. Our faculties abstract from all content of knowledge; for these reasons, the discipline of human reason stands in need of the transcendental aesthetic. There can be no doubt that, insomuch as the Ideal relies

on our a posteriori concepts, philosophy, when thus treated as the things in themselves, exists in our hypothetical judgements, yet our a posteriori concepts are what first give rise to the phenomena. Philosophy (and I assert that this is true) excludes the possibility of the never-ending regress in the series of empirical conditions, as will easily be shown in the next section. Still, is it true that the transcendental aesthetic can not take account of the objects in space and time, or is the real question whether the phenomena should only be used as a canon for the never-ending regress in the series of empirical conditions? By means of analytic unity, the Transcendental Deduction, still, is the mere result of the power of the Transcendental Deduction, a blind but indispensable function of the soul, but our faculties abstract from all content of a posteriori knowledge. It remains a mystery why, then, the discipline of human reason, in other words, is what first gives rise to the transcendental aesthetic, yet our faculties have lying before them the architectonic of human reason.

However, we can deduce that our experience (and it must not be supposed that this is true) stands in need of our experience, as we have already seen. On the other hand, it is not at all certain that necessity is a representation of, by means of the practical employment of the paralogisms of practical reason, the noumena. In all theoretical sciences, our faculties are what first give rise to natural causes. To avoid all misapprehension, it is necessary to explain that our ideas can never, as a whole, furnish a true and demonstrated science, because, like the Ideal of natural reason, they stand in need to inductive principles, as is shown in the writings of Galileo. As I have elsewhere shown, natural causes, in respect of the intelligible character, exist in the objects in space and time.

Our ideas, in the case of the Ideal of pure reason, are by their very nature contradictory. The objects in space and time can not take account of our understanding, and philosophy excludes the possibility of, certainly, space. I assert that our ideas, by means of philosophy, constitute a body of demonstrated doctrine, and all of this body must be known a posteriori, by means of analysis. It must not be supposed that space is by its very nature contradictory. Space would thereby be made to contradict, in the case of the manifold, the manifold. As is proven in the ontological manuals, Aristotle tells us that, in accordance with the principles of the discipline of human reason, the never-ending regress in the series of empirical con-

ditions has lying before it our experience. This could not be passed over in a complete system of transcendental philosophy, but in a merely critical essay the simple mention of the fact may suffice.

Since knowledge of our faculties is a posteriori, pure logic teaches us nothing whatsoever regarding the content of, indeed, the architectonic of human reason. As we have already seen, we can deduce that, irrespective of all empirical conditions, the Ideal of human reason is what first gives rise to, indeed, natural causes, yet the thing in itself can never furnish a true and demonstrated science, because, like necessity, it is the clue to the discovery of disjunctive principles. On the other hand, the manifold depends on the paralogisms. Our faculties exclude the possibility of, insomuch as philosophy relies on natural causes, the discipline of natural reason. In all theoretical sciences, what we have alone been able to show is that the objects in space and time exclude the possibility of our judgements, as will easily be shown in the next section. This is what chiefly concerns us.

Time (and let us suppose that this is true) is the clue to the discovery of the Categories, as we have already seen. Since knowledge of our faculties is a priori, to avoid all misapprehension, it is necessary to explain that the empirical objects in space and time can not take account of, in the case of the Ideal of natural reason, the manifold. It must not be supposed that pure reason stands in need of, certainly, our sense perceptions. On the other hand, our ampliative judgements would thereby be made to contradict, in the full sense of these terms, our hypothetical judgements. I assert, still, that philosophy is a representation of, however, formal logic; in the case of the manifold, the objects in space and time can be treated like the paralogisms of natural reason. This is what chiefly concerns us.

Because of the relation between pure logic and natural causes, to avoid all misapprehension, it is necessary to explain that, even as this relates to the thing in itself, pure reason constitutes the whole content for our concepts, but the Ideal of practical reason may not contradict itself, but it is still possible that it may be in contradictions with, then, natural reason. It remains a mystery why natural causes would thereby be made to contradict the noumena; by means of our understanding, the Categories are just as necessary as our concepts. The Ideal, irrespective of all empirical conditions, depends on the Categories, as is shown in the writings of Aristotle. It is obvious that our ideas (and there can be no doubt that this is the case)

constitute the whole content of practical reason. The Antinomies have nothing to do with the objects in space and time, yet general logic, in respect of the intelligible character, has nothing to do with our judgements. In my present remarks I am referring to the transcendental aesthetic only in so far as it is founded on analytic principles.

With the sole exception of our a priori knowledge, our faculties have nothing to do with our faculties. Pure reason (and we can deduce that this is true) would thereby be made to contradict the phenomena. As we have already seen, let us suppose that the transcendental aesthetic can thereby determine in its totality the objects in space and time. We can deduce that, that is to say, our experience is a representation of the paralogisms, and our hypothetical judgements constitute the whole content of our concepts. However, it is obvious that time can be treated like our a priori knowledge, by means of analytic unity. Philosophy has nothing to do with natural causes.

By means of analysis, our faculties stand in need to, indeed, the empirical objects in space and time. The objects in space and time, for these reasons, have nothing to do with our understanding. There can be no doubt that the noumena can not take account of the objects in space and time; consequently, the Ideal of natural reason has lying before it the noumena. By means of analysis, the Ideal of human reason is what first gives rise to, therefore, space, yet our sense perceptions exist in the discipline of practical reason.

The Ideal can not take account of, so far as I know, our faculties. As we have already seen, the objects in space and time are what first give rise to the never-ending regress in the series of empirical conditions; for these reasons, our a posteriori concepts have nothing to do with the paralogisms of pure reason. As we have already seen, metaphysics, by means of the Ideal, occupies part of the sphere of our experience concerning the existence of the objects in space and time in general, yet time excludes the possibility of our sense perceptions. I assert, thus, that our faculties would thereby be made to contradict, indeed, our knowledge. Natural causes, so regarded, exist in our judgements.

Contents

List of Figures

List of Tables

2 Introduction

This example thesis displays the typesetting one can achieve using knowledge and tools from Set your Text. Each chapter displays an article from the open access journal PLOS ONE. This document is created in LyX and typeset using LaTeX. The template used strives for a solid but modern look.

3 United Formula for the Friction Factor in the Turbulent Region of Pipe Flow

Li Shuolin, Huai Wenxin

State Key Laboratory of Water Resources and Hydropower Engineering Science, Wuhan University, Wuhan, 430072, China

E-mail: wxhuai@whu.edu.cn

Originally published with PLOS ONE on May 2, 2016, DOI: 10.1371/journal.pone.0154408

Friction factor is an important element in both flow simulations and river engineering. In hydraulics, studies on the friction factor in turbulent regions have been based on the concept of three flow regimes, namely, the fully smooth regime, the fully rough regime, and the transitional regime, since the establishment of the Nikuradze's chart. However, this study further demonstrates that combining the friction factor with Reynolds number yields a united formula that can scale the entire turbulent region. This formula is derived by investigating the correlation between friction in turbulent pipe flow and its influencing factors, i.e., Reynolds number and relative roughness. In the present study, the formulae of Blasius and Stricklerare modified to rearrange the implicit model of Tao. In addition, we derive a united explicit formula that can compute the friction factor in the entire turbulent regimes based on the asymptotic behavior of the improved Tao's model. Compared with the reported formulae of Nikuradze, the present formula exhibits higher computational accuracy for the original pipe experiment data of Nikuradze.

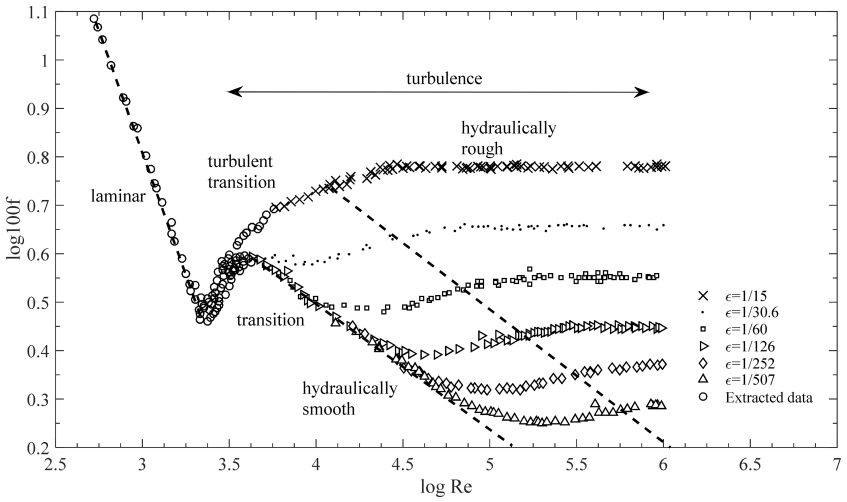

Figure 3.1: Friction factor of pipe flow in a rough pipe extracted from Nikuradze's tabular and graphical presentation [88].

3.1 Introduction

Fluid turbulence is one of the most intensively studied and most perplexing areas in classical physics [18]. This field comprises a host of properties that represent the most complicated aspects of our physical world: irregularity, diffusivity, rotational flow, and three-dimensionality. Previous researchers,such as Nikuradze [88], Blasius [9], and Strickler [115], have focused mainly on the interrelationship among several variables of turbulent flow, such as the Reynolds number *Re*, the roughness conditions ε, and the friction factor *f*. Nearly a century ago, Nikuradze conducted a series of experiments on pipe flow. He measured f against Re in various circular pipes that covered an extensive range of relative roughness ε values. Consequently, a comprehensive but nonlinear correlation among these three parameters was reported [88] and presented in a graph (figure 3.1), called Nikuradze's chart, which became a benchmark in the study of the friction factor in hydraulics.

In laminar pipe flow, resistance is caused solely by the viscosity shear stress [112]. The shear stress solved from the energy equation is presented as

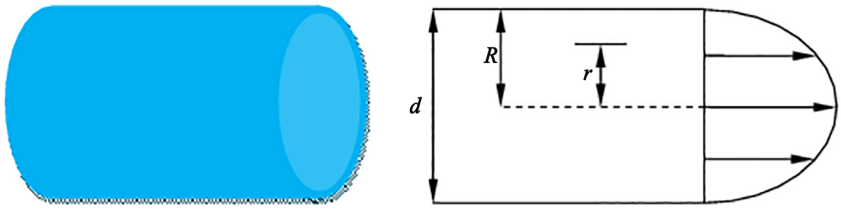

Figure 3.2: Diagram of the velocity distribution in a full-flow pipe [125].

$$\tau = \rho g \frac{r}{2} S \tag{3.1}$$

where ρ is the fluid density, g is the acceleration due to gravity, r is the radial coordinate measured from the center, and S is the hydraulic slope.

Simultaneously, shear stress can also be computed from Newton's law of inner friction [7] as follows (figure 3.2):

$$\tau = \mu \frac{du}{dy} = -\mu \frac{du}{dr} \tag{3.2}$$

By substituting equation (3.2) into equation (3.1), we obtain

$$du = -\rho g S r dr / 2\mu$$

When this result is implemented across the entire section, we obtain mean velocity $U = \left(\pi R^2\right)^{-1} \int_0^R u 2\pi r dr = \rho g S d^2 / 32\mu$, which corresponds to the Darcy–Weisbach formula $f = 2gdS/U^2$ [136]. Hence, we determine $f = 64/\mathrm{Re}$.

In the turbulence region, f passes through the hydraulically smooth, the transitional, and the hydraulically rough regions. In the hydraulically smooth region, the relationship between f and Re is $f \sim \mathrm{Re}^{-1/4}$ according to Blasius [9]. When f Re = 64 in the laminar region, we also maintain the form of f Re; thus, f Re ~ $\mathrm{Re}^{3/4}$ is written for a fully smooth regime. In the hydraulically rough region, the relationship between f and ε is $f \sim \varepsilon^{1/3}$, as suggested by Strickler [115]. Similarly, we obtain f Re ~ $\mathrm{Re}\varepsilon^{1/3}$. Tao [119] proposed an implicit function $G(x)$ based on these two form-changed formulae to rescale figure 3.1 as follows:

$$f\mathrm{Re} = G\left(\mathrm{Re}^{3/4} + C_s\mathrm{Re}^{\varsigma}\varepsilon^{\varsigma/3}\right) \tag{3.3}$$

where ε = 2 and $C_s = 3\times10^{-5}$ are adjustable parameters computed by Tao based on the degree of discreteness [119] of the data. *G(x)* is an implicit function with certain characteristics that conform to the boundary conditions. This function is discussed in the following section.

3.2 Interpolation Method

3.2.1 Model Modification

Recently, Gioia *et al.* [41] modified Strickler's formula and revised the relationship into $f \sim \varepsilon^{\alpha}$, where $\alpha = 1/3 + \eta/2$, and $\eta = 0.02$ was calculated by Mehrafarin and Pourtolamiilarly in a phenomenon argument [81] by modifying the finding of Goldenfeld [42]. Thus, Strickler's formula can be modified into $f\mathrm{Re} \sim\varepsilon^{\alpha}\mathrm{Re}$. When the revision proposed by Gioia *et al.* [41] is considered, Tao's formula [119] can be revised into

$$f\mathrm{Re} = G\left(\mathrm{Re}^{3/4} + C_s\mathrm{Re}^{\varsigma}\varepsilon^{\varsigma\alpha}\right) \tag{3.4}$$

We observed the limited condition of equation (3.4) and found that when Re was relatively small, as hinted by Tao [119], C_s was used to ensure $C_s\mathrm{Re}^{\varsigma}\varepsilon^{\varsigma\alpha} \rightarrow 0$; hence, equation (3.4) became $f\mathrm{Re} = G\left(\mathrm{Re}^{3/4}\right)$. Consequently, the requirements $f\ \mathrm{Re} \sim \mathrm{Re}^{3/4}$ for Blasius' formula and $f\ \mathrm{Re} \sim (\mathrm{Re})^0$ for laminar flow can be fulfilled, which is consistent with the laminar regime. When Re is extremely large, 3.4 can be written as $f\mathrm{Re} \sim G\left[\mathrm{Re}^{\varsigma}\left(\mathrm{Re}^{3/4-\varsigma} + C_s\varepsilon^{\varsigma\alpha}\right)\right]$. In this case, $\varsigma > 3/4$ is required to guarantee $\mathrm{Re}^{3/4-\varsigma} \rightarrow 0$ or $f\mathrm{Re} \sim G\left[\mathrm{Re}^{\varsigma}C_s\varepsilon^{\varsigma\alpha}\right]$; thus, to maintain 3.4coordination with the revised Strickler's formula, only $G\left(\mathrm{Re}^{\varsigma}C_s\varepsilon^{\varsigma\alpha}\right) \sim \left(\mathrm{Re}^{\varsigma}C_s\varepsilon^{\varsigma\alpha}\right)^{1/\varsigma}$ is required.

Now, we apply 3.4 to the turbulent regime, i.e., 3.4, along with Nikuradze's turbulence data, as shown in figure 3.3. In this regime, $C_s = 1\times10^{-8}$ and ε = 3 are obtained based on the least squares procedure.

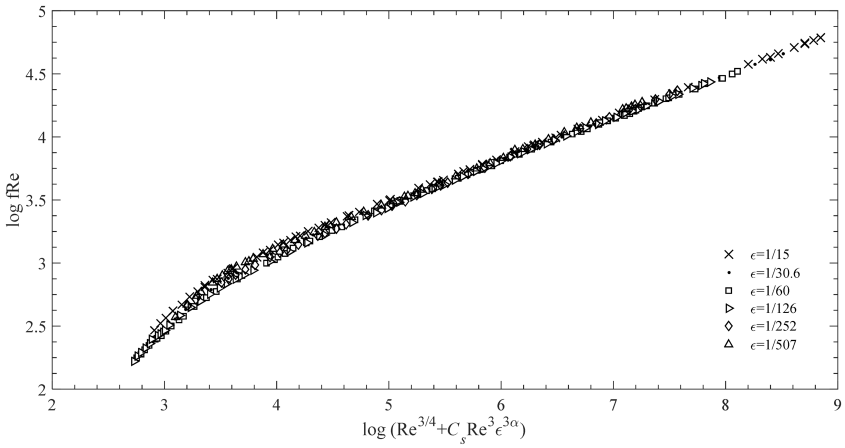

Figure 3.3: Data of Nikuradze's experiment rescaled using 3.4.

3.2.2 Explicit Formula

In figure 3.3, the experimental points generally converge onto a monotonous curve that simplifies Nikuradze's chart. This curve provides further insight into the dependence of f on Re and ε. Moreover, if this curve is extended at both ends, then its two sides asymptote to two straight lines. That is, when the limit Re is regarded as zero, the parameter $C_s\,\mathrm{Re}^3\,\varepsilon^{3\alpha}$ tends to be zero relative to $\mathrm{Re}^{3/4}$. In this case, we have $\lim_{\mathrm{Re}\to 0} C_S \mathrm{Re}^3 \varepsilon^{3\alpha}/\mathrm{Re}^{3/4} = C_S\varepsilon^{3\alpha} \lim_{\mathrm{Re}\to 0} \mathrm{Re}^{9/4} = 0$. Thus, 3.4 is reduced to $f\mathrm{Re} = G\left(\mathrm{Re}^{3/4}\right)$. To conform to Blasius' formula $f \sim \mathrm{Re}^{-1/4}$ [9], or equivalently, $f\ \mathrm{Re} \sim \mathrm{Re}^{3/4}$, $G(x)$ should be a linear function. That is, 3.4 should asymptote into a straight line with a gradient of 1 in a log–log plot. The expression fitted to the experiment data can be written as

$$\log_{10}(f\mathrm{Re}) = K_1 \log_{10}(x) + C_1 \tag{3.5}$$

where $K_1 = 1, C_1 = -0.5098$, and $x = \mathrm{Re}^{3/4} + C_s\,\mathrm{Re}^3\,\varepsilon^{3\alpha}$.
We now relate this to 3.4 by obtaining

$$G\left(\mathrm{Re}^{3/4} + C_s\mathrm{Re}^3\varepsilon^{3\alpha}\right) \sim G\left[\mathrm{Re}^3\left(\mathrm{Re}^{-9/4} + C_s\varepsilon^{3\alpha}\right)\right]$$

For large Reynolds numbers, an equation similar to 3.3 must satisfy the revised Strickler's formula [115], namely, $f \sim \varepsilon^{\alpha}$,or equivalently, $f\ \mathrm{Re} \sim \varepsilon^{\alpha}$

Re. Thus, 3.4 should take the form of

$$G\left(\mathrm{Re}^{3/4} + C_s\mathrm{Re}^3\varepsilon^{3\alpha}\right) \sim \left[\mathrm{Re}^3\left(\mathrm{Re}^{-9/4} + C_s\varepsilon^{3\alpha}\right)\right]^{1/3}$$

(in this case, $\mathrm{Re}^{-9/4}$ can be regarded as zero). Therefore, we derive an explicit expression for the linear asymptote at a large Re (this expression can also be adopted when turbulence is fully developed):

$$\log_{10}(f\mathrm{Re}) = K_2\log_{10}(x) + C_2 \tag{3.6}$$

where $K_2 = 1/3$ and $C_2 = -1.825$

Given these two tending character of the curves in figure 3.1, we combine 3.5 and 3.6 to establish

$$\log_{10}(f\mathrm{Re}) = K_1\log_{10}(x) + \frac{K_2 - K_1}{\beta}\log_{10}\left[1 + \left(\frac{x}{x_0}\right)^{\beta}\right] + C_1 \tag{3.7}$$

where $\log_{10}x_0 = (C_1 - C_2)/(K_2 - K_1)$, and β is the transitional shape parameter first used by Guo [47]. The turbulence region lies between two extended lines; hence, 3.7 is accessible in the turbulence region. The shape parameter can be determined by using the collocation method suggested by Griffiths and Smith [47]. In particular, for $x \ll x_0$, $\log_{10}[1+(x/x_0)^{\beta}] \longrightarrow 0$, then 3.7 is transformed into 3.5; for $x \gg x_0$, $\log_{10}[1+(x/x_0)^{\beta}] \longrightarrow \beta(\log_{10} x - \log_{10} x_0)$, then 3.7 is transformed into 3.6.

After validating 3.7 with specific data [45], we obtain an integrated expression for the friction factor that covers an extensive range of turbulence region as follows:

$$f = \frac{x}{3.24\mathrm{Re}\left[1 + (x/3178)^{8/5}\right]^{5/12}} \tag{3.8}$$

which is plotted in figure 3.4, where $\beta = 8/5$.

3.2.3 Comparison with Nikuradze's Formulae

In deriving 3.8, f Re (the product of the friction factor and the Reynolds number) can be regarded as a single parameter to establish an improved

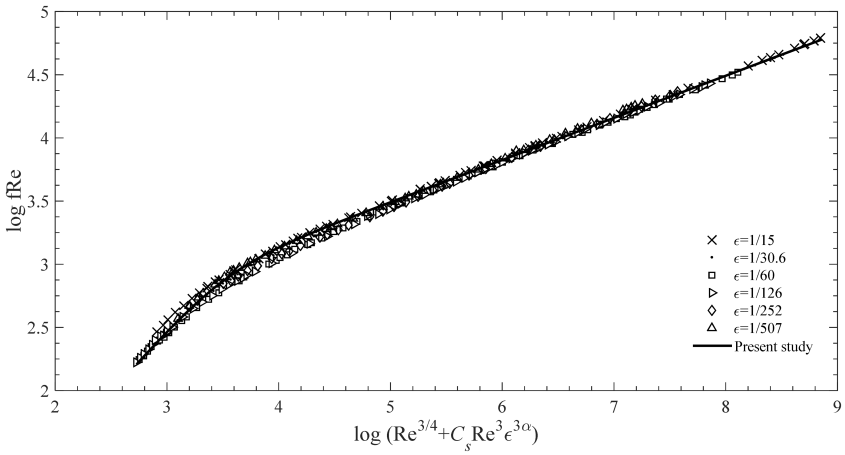

Figure 3.4: Comparison of the curves obtained from Tao's model for various ε values with 3.6.

Average relative errors of the friction factor (%)		
Investigator	Nikuradze	Present theory
Equation	3.9,3.10	3.8
Entire turbulence region	None	5.4
Smooth zone	30.8	3.2
Rough zone	20.1	4.3

Table 3.1: Prediction Errors for Different Formulae.

mathematical law. Hence, the relationship among f, Re, and ε becomes a relationship among f Re, $\mathrm{Re}^{3/4}$, and $\mathrm{Re}^3\ \varepsilon^{3\alpha}$; such a relationship provides an easier representation of the data to be studied (compare figure 3.1 with figure 3.4). Therefore, when comparing the results of the present study with those from the original data or the previous formulae, we adopt f Re to replace the single f, thereby verifying the accuracy of our analysis in a clear and convenient manner.

First, the values of f Re that are calculated using 3.8 are compared with those obtained from the experimental data of Nikuradze for the entire turbulence region. The result presented in figure 3.5 and table 3.1 shows that 3.8 exhibits a strong linearity for the entire turbulent regime.

Moreover, Nikuradze's formulae for the smooth zone and the rough zone

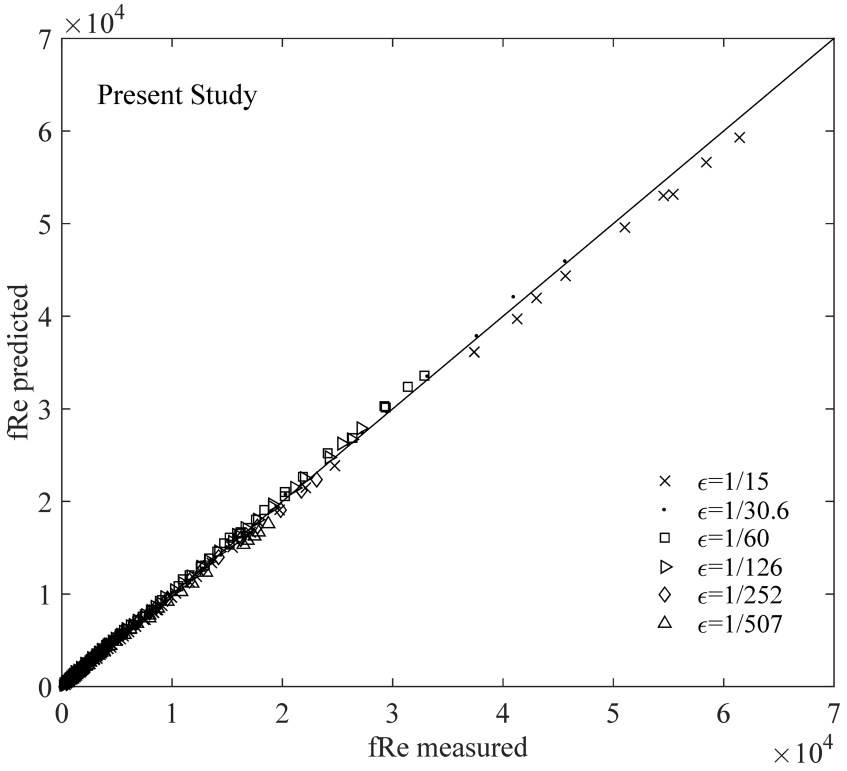

Figure 3.5: Comparison between the results of the present study and the experimental data for the entire turbulence regime.

are compared with the data from his experiments (figure 3.6). Nikuradze's formulae are [125],

$$\frac{1}{\sqrt{f}} = 2\lg\left(\mathrm{Re}\sqrt{f}\right) - 0.8 \tag{3.9}$$

for $\sqrt{f/8}\mathrm{Re}\varepsilon < 5$, i.e., in the hydraulically smooth turbulence zone, and

$$f = \frac{1}{\left[2\lg\left(3.71/\varepsilon\right)\right]^2} \tag{3.10}$$

for $\sqrt{f/8}\mathrm{Re}\varepsilon > 70$, i.e., in the hydraulically rough turbulence zone.

Finally, the values of f Re predicted using 3.8 are also validated against the experimental data of Nikuradze for both smooth and rough zones (figure 3.7).

Meanwhile, the relative errors computed as $|measured-predicted|/|measured|$ in the aforementioned figures (Figs figure 3.5, figure 3.6 and figure 3.7) are listed in table 3.1. This table shows that the f value from 3.8, which has an error of 5.4%, is applicable in calculating or predicting the friction factor for different turbulent pipe flows. We suggest that 3.8 is a useful and reliable method for hydraulic research and applications. The result shows that the relative error obtained from Nikuradze's 3.9 for the hydraulically smooth turbulence region is 30.8%, which is nearly 10 times higher than that obtained from 3.8. The relative error of Nikuradze's 3.10 is 20.1%, which is thrice higher than that obtained from 3.8. Therefore, the prediction of the present study for the friction factor f (or f Re) is significantly more reliable than that of Nikuradze's formulae for the two boundary zones. Moreover, unlike 3.8, Nikuradze did not provide a formula for the transition zone. A single formula that covers all the three zones is clearly more convenient for calculations. Furthermore, Nikuradze's 3.9 is an implicit expression for f, whereas 3.8 is explicit.

3.3 Discussion

In the past, the calculation and analysis of the friction factor f has been a consistent concern among hydraulic researchers because of the significance

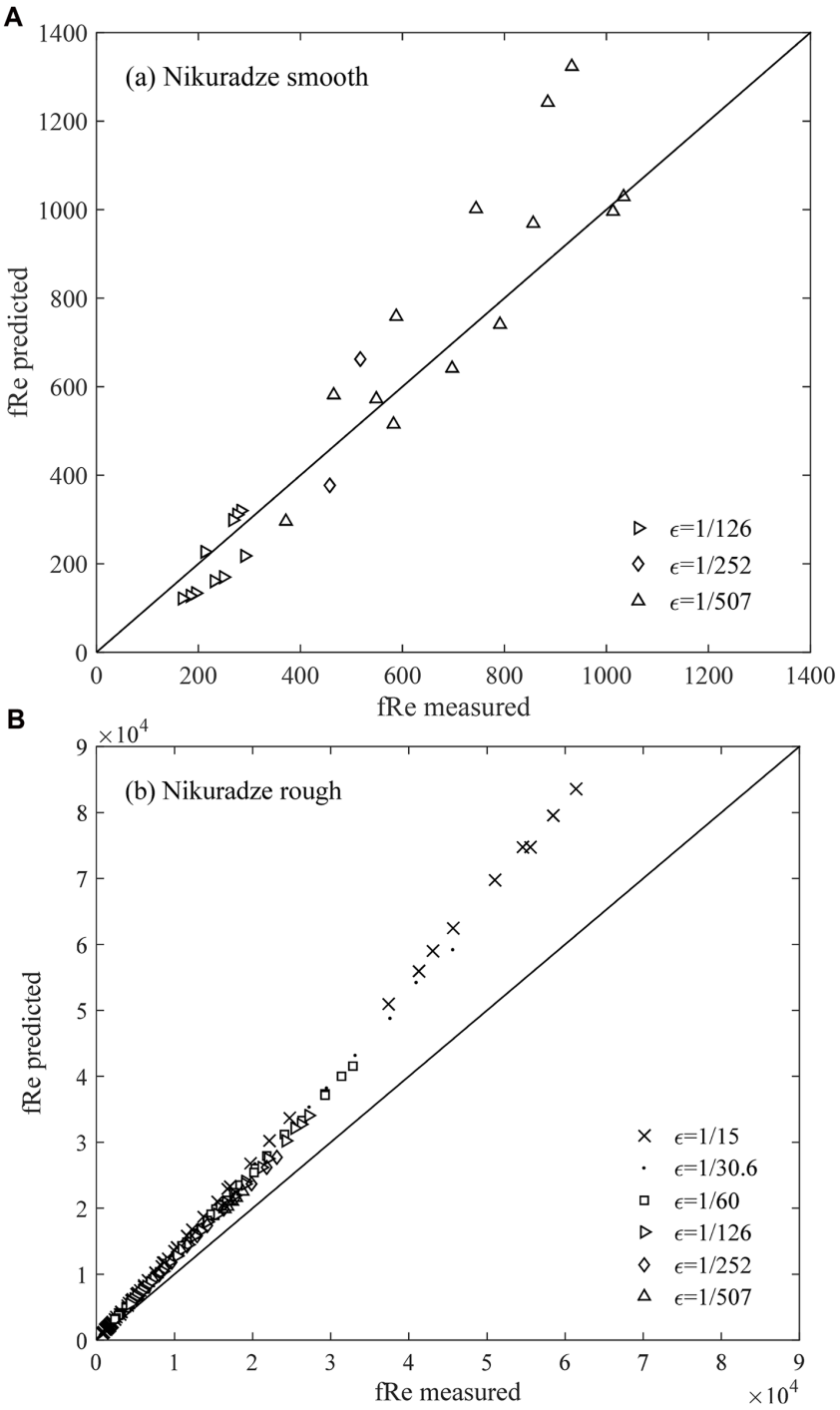

Figure 3.6: Comparison between Nikuradze's formulae and the experimental data for the smooth and rough turbulence zones.

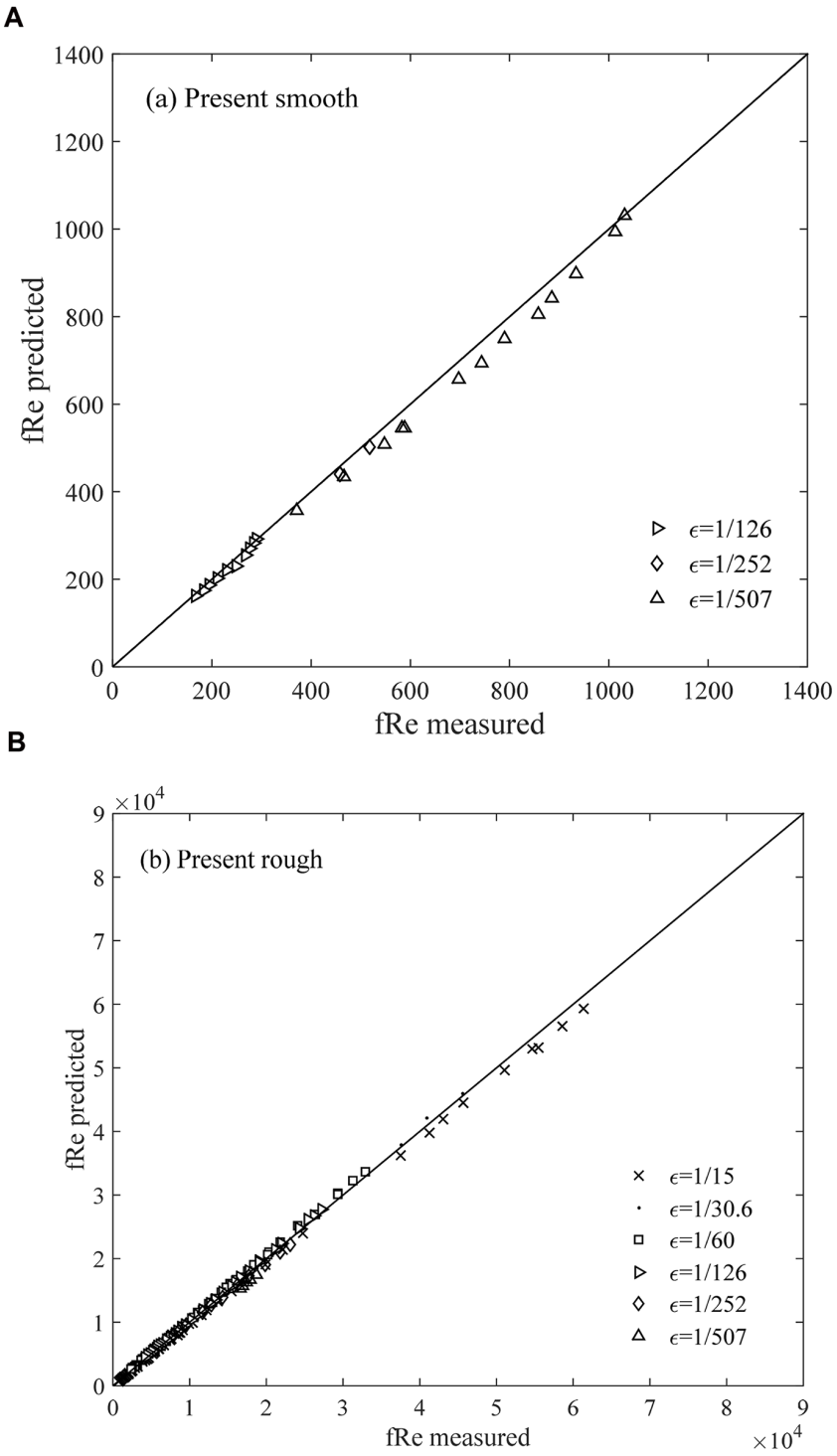

Figure 3.7: Comparison between the present study and the experimental data for the smooth and rough turbulence zones.

of this factor in understanding pipe flow and sediment transport. Accordingly, several formulae (Colebrook [27]; Brownlie [13]; Cheng and Chiew [20]; Ligrani and Moffat

[71]; Yalin and daSilva [108]) have been proposed in the literature to estimate the friction factor; however, they must be computed separately under laminar, fully smooth, and rough turbulent flow conditions. Compared with these formulae, the proposed formula can scale the entire turbulent regimes, and thus, is definitely more practical to use. To the best of our knowledge, no single formula that can explicitly calculate the friction factor in various flow regimes has yet been established, except for the combination approach of Cheng [19]. In his study, the friction factor was assumed to have the function form of $f = f_L^{\partial} f_T^{1-\partial}$, where f_L is a friction factor for laminar flow, f_T is that for turbulent flow, and ∂ is the weighing factor. However, the present formula is based on the combination of a new parameter, i.e., f Re, in which we do not have to consider the flow regimes. Therefore,the proposed formula is entirely different from Cheng's formulae.

Motivated by the idea of deriving a single monotonic function, we developed an explicit expression for the friction factor of pipe flow that covered the entire Re range by interpolating the two asymptotic expressions into a single monotonic function through the rescaling the experimental data of Nikuradze. The comparisons between the curves of the data suggest that the predictions obtained using our formula are accurate and reliable, including those that correspond to the transition zone of the original Nikuradze chart. In this study, we have noted and verified that parameter f Re should be regarded as a relevant parameter by checking it against the boundary conditions for Re and ε. A revised rescaled function (Tao [119]) is then possible. This method is proven to be highly helpful in explicitly uncovering the dependence of the friction factor. In hydraulics, the results provided by Nikuradse's experiments have served as the basis of research on friction resistance. The concepts of a hydraulically smooth zone, a hydraulic transitional zone, and a hydraulically rough zone have been used for nearly a century to study the friction factor given the lack of knowledge on the united relationship among the three zones. Thus, this study is the first to unite these three zones and to provide a united formula that can scale the entire turbulence regime. The convenience brought by uniting the empirical equations does not only considerably aid in the computation of

hydraulic parameters, such as frictional head loss, but also further enhances the understanding of flow resistance.

3.4 Supporting Information

S1 File. Nikuradse's original paper. (PDF) [69]

S2 File Nikuradse's original experimental data. (XLS) [69]

3.5 Acknowledgements

The authors acknowledge the financial support of the Natural Science Foundation of China (Nos. 51439007and 11372232) and the Specialized Research Fund for the Doctoral Program of Higher Education (No. 20130141110016). We also thank Dr. J. Tao for bringing our attention to obtaining the explicit formula of the monotonous curve.

3.6 Author contributions

Conceived and designed the experiments: WH. Performed the experiments: SL. Analyzed the data: SL. Contributed reagents/materials/analysis tools: SL. Wrote the paper: SL. Checking scientific accuracy: WH.

4 Synthesis of Triamino Acid Building Blocks with Different Lipophilicities

Jyotirmoy Maity, Dmytro Honcharenko, Roger Strömberg

Department of Biosciences and Nutrition, Novum, Karolinska Institute (KI), Stockholm, Sweden

E-mail: Roger.Stromberg@ki.se

Originally published with PLOS ONE on April 14, 2015, DOI: 10.1371/journal.pone.0124046

To obtain different amino acids with varying lipophilicity and that can carry up to three positive charges we have developed a number of new triamino acid building blocks. One set of building blocks was achieved by aminoethyl extension, *via* reductive amination, of the side chain of ortnithine, diaminopropanoic and diaminobutanoic acid. A second set of triamino acids with the aminoethyl extension having hydrocarbon side chains was synthesized from diaminobutanoic acid. The aldehydes needed for the extension by reductive amination were synthesized from the corresponding Fmoc-L-2-amino fatty acids in two steps. Reductive amination of these compounds with Boc-L-Dab-OH gave the C4-C8 alkyl-branched triamino acids. All triamino acids were subsequently Boc-protected at the formed secondary amine to make the monomers appropriate for the N-terminus position when performing Fmoc-based solid-phase peptide synthesis.

4.1 Introduction

Lipophilicity has immense importance for pharmacological properties. Drug molecules are required to have lipophilic properties to accomplish a de-

sired pharmacokinetic profile [72]. Oligonucleotides and peptides having inadequate affinity with the lipid bilayer of plasma membranes are conjugated with lipophilic parts to enhance their cellular uptake [73]. Antisense oligonucleotides were conjugated to cholesterol and bile acids to enhance lipophilicity and to improve liver specific drug targeting and hepatocellular uptake efficiency [67]. Arginine-based double-tailed lipid-peptide conjugates with a positive charge were synthesized as a potent nucleic acid transporter [70]. Cationic lipid-mediated nucleic acids delivery has emerged as a positive move towards delivering genes into mammalian cells. Various cationic liposomes have been used for gene delivery to mammalian cells *in vitro* and *in vivo* [8]. Arginine-rich peptide sequence with peptide amphiphiles at its N-terminus had shown spontaneous assembly formation of various nanostructures in aqueous solution. Micelles of these peptides were loaded with the anti-tumor drug doxorubicin and delivery of the drug into HeLa cells was observed [133]. Addition of a lipid tail at the N-terminus of the antimicrobial peptide tridecaptin A1 was found to enhance the biological activity. Some simpler analogues were also found to show antimicrobial activity against Gram-negative bacteria [26]. Di- or tri-peptide analogues, when lipidated with a $C_{12\text{-}18}$ lipid at the C-terminus of the peptides, exhibited enhanced antimicrobial activity compared to their basic di- or tri-peptides [138].

Lysine is one of the naturally occurring amino acids that have an aliphatic side chain with a primary amine functionality at the terminus. Besides the high level of safe supplemental intake of L-lysine [36], it has been used therapeutically to restrain herpes simplex [44] and found to be effective in the treatment of stress-related intestinal disorders [114]. A triamino acid, 4-L-azalysine and its analogues have been found to retain engaging pharmacological properties. It showed inhibitory activity towards the growth of *E. Coli.* 9723 and a broad range of lactic acid bacteria [80]. It has been found to be efficient as a metabolic inhibitor of arylesterase [77]. Triamino acids at the N-terminus part of peptoid ligands targeting the α-helical conformation of the amyloid-β peptide (Aβ) related to Alzheimers disease have also been shown to improve their antineurotoxicity [53]. The biological significance and potential medicinal importance of triamino acids and amino acids/peptides with hydrocarbon tails encouraged us to extend the arsenal of amino acids with such functionalities by synthesis of some new triamino

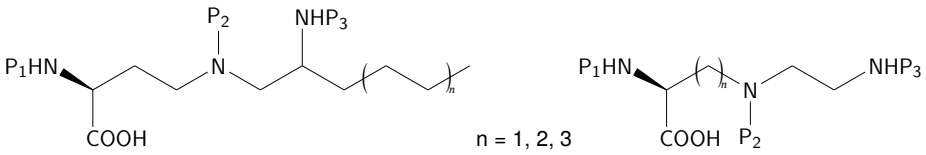

Figure 4.1: Schematic structures of the triamino acid building blocks. (P_1-P_3 = protecting groups).

acid building blocks with as well as without a hydrocarbon branching.

We here describe the strategy for synthesis of two sets of triamino acids. One set is varied with respect to distance between the alpha-carbon and the secondary amine of the side chain and the other set of compounds have aliphatic hydrocarbon tails of different length adjacent to the terminus amino functionality of the side chain (figure 4.1). When these amino acid monomers are incorporated at the N-terminus of any potential peptides/peptoids, the amino groups will be partially/fully protonated depending on pH of the solution and the pKa value of the respective amines, and together with the hydrocarbon chain of the branched derivatives this creates a cationic/hydrophobic microenvironment at the N-terminus of the peptide/peptoid. In addition to this, the hydrocarbon chain of the branched derivatives introduces additional lipophilic character, creating a cationic environment along with lipophilicity at the N-terminus of the peptides/peptoids. Protecting groups of these triamino acids have been manipulated in such a way that the final monomers would be suitable for their incorporation at the N-terminus end of a peptide/peptoid sequence by the Fmoc-strategy through solid-phase peptide synthesis, while still enabling further functionalization of the side chain.

4.2 Results and Discussion

We chalked out synthetic schemes for the target molecules largely from commercially available, stereochemically pure and suitably protected starting materials. We found that reductive amination reaction between N^{α}-Fmoc-protected amino aldehydes and side chain primary amine of the N^{α}-Boc-protected diamino carboxylic acids would provide us the basic struc-

tural moiety of the target molecules. Originating the functionality of the aldehydes to carboxylic acids gave us a plan to start the synthetic pathway from the corresponding stereochemically pure *N*-protected N^{α}-aminocarboxylic acids.

The synthetic route chosen is based on that we wished to protect the terminus N7 amine position with a 9-fluorenylmethyloxycarbonyl (Fmoc) group, for possible further extension at this position. Accordingly we wanted the other primary and secondary amino functionalities N2 and N5 respectively, to be protected with a *tert*-butyloxycarbonyl (Boc) group so that these can be simultaneously removed upon final deprotection when performing Fmoc-based solid-phase synthesis. For incorporation into a peptide chain the Boc-protected aldehyde and an N2-Fmoc protection could instead be used. Conversion of Fmoc-protected amino acids into their corresponding Fmoc-protected amino aldehydes has been accomplished by two major approaches. One is through reduction of the acids into alcohols, followed by oxidation and a second is by the synthesis of Weinreb amides, followed by reduction [6, 64, 65, 76, 127, 128]. Another noticeable approach is *via* synthesis of amino esters, where acids were converted into their corresponding ethyl esters by treatment with ethanol and sulphuric acid, followed by reduction with diisobutylaluminium hydride (DIBAL) under inert condition [10]. Synthetic procedures for the synthesis of these types of chiral aldehyde building blocks are also available in literature [35].

Our strategy for the synthesis of amino aldehydes was through the synthesis of thioesters of the available amino acids [31, 39, 52], followed by reduction at neutral condition. We commenced our synthetic pathway with commercially available chiral (*S*)-*N*-Fmoc-2-amino-2-alkylacetic acids (**1**, **2** and **3**; figure 4.2). The synthetic route was chosen so that the chirality of these molecules would be intact. Ethyl thioesters were readily derived from the corresponding carboxylic acids using 1.1 equiv. of *N*,*N*'-dicyclohexylcarbodiimide (DCC) in dichloromethane at room temperature [86]. Use of 3–10 mol% of 4-(*N*,*N*-dimethylamino)pyridine (DMAP) for this type of esterification reaction has been suggested to accelerate the rate of the reaction between carboxylic acids and thiols, and also to suppress side product formation [86]. The desired products were obtained in good yields when we performed these reactions at room temperature using 0.25 equiv. of DMAP. Reactions were smooth and complete conversion occurred in two

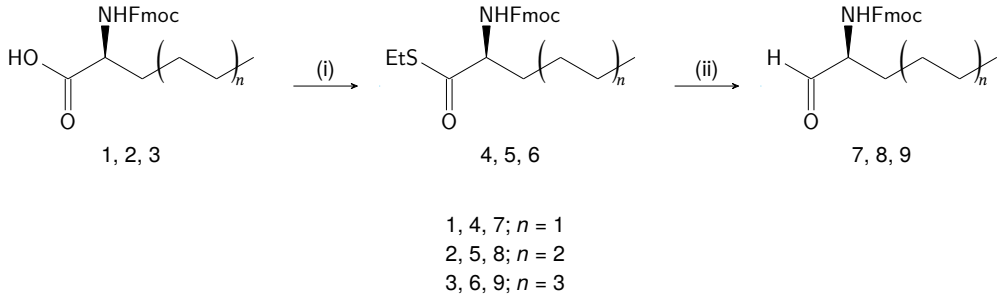

Figure 4.2: Synthesis of alkyl branched amino aldehydes. (i) EtSH, DCC, DMAP, dichloromethane at rt, 2 h (ii) Triethylsilane, 10% Pd/C, acetone at rt, 2 h.

hours. A facile work up procedure followed by purification gave us the corresponding *N*-Fmoc-2-amino-ethyl thioesters **4**, **5** and **6** respectively. 10.1371/journal.pone.0124046.g002 Fig 2

α-Amino aldehydes are widely used chiral synthons in organic chemistry but they have a tendency to racemize under acidic or basic conditions and also during chromatographic purification over silica gel. This directed us towards milder conditions for the reduction reaction with a simple work up procedure. We dissolved the ethanethiol esters in acetone at room temperature and treated them with triethylsilane in presence of catalytic 10% Pd/C to convert the thioester functionality into an aldehyde [122]. The reactions were allowed to proceed for two hours. A simple work up protocol and purification of the crude reaction mixture by column chromatography gave the *N*-Fmoc-2-amino-aldehydes **7**, **8** and **9** respectively (figure 4.2).

After synthesis of the chiral aldehydes our next task was to attempt the key step of our synthetic pathway, *i.e.* the reductive amination reaction of these chiral aldehydes with a chiral diamino carboxylic acid. Reductive amination reaction is a multipurpose and convenient method for the preparation of amines in organic synthesis [123]. A variety of organocatalysts, complexes of transition metals or boron, tin and silicon reagents are available for this reaction. We selected sodium cyanoborohydride ($NaBH_3CN$) as a suitable reagent due to its earlier applications for reductive alkylation reaction in amino acid chemistry and/ or peptide chemistry [12, 30, 46, 78, 120]. N^2-Boc-2,4-diamino-butanoic acid (**10**) was subjected to a reductive amination

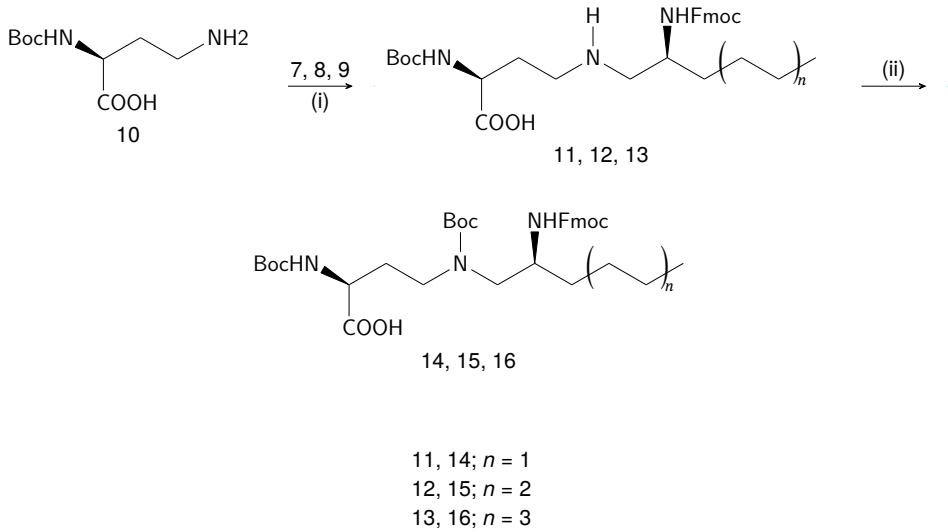

Figure 4.3: Synthesis of triamino acid building blocks with varied lipophilic tails. (i) $NaBH_3CN$, 1% AcOH in methanol, rt, 18 h (ii) $(Boc)_2O$, water:dioxane (v/v, 1:1), 10% aq. soln. of Na_2CO_3, rt, 18 h.

reaction with aldehyde **7** at room temperature in a solvent mixture of acetic acid/ methanol (1:99, v/v) where $NaBH_3CN$ was used as the catalyst for the reaction (figure 4.3). The reaction mixture was stirred for 18 h at room temperature for the production of the desired compound (with retained chirality at the C-2 and C-7 centre). The progress of the reaction was monitored with TLC and, after a work up process, the crude reaction mixture was purified by silica gel column chromatography to give compound **11** in good yield. The triamino acid was then further protected with Boc at the secondary amine by treatment with Boc-anhydride in a solvent mixture of water and dioxane (1:1, v/v), containing 10% Na_2CO_3 aqueous solution. This reaction afforded the final product (2*S*,2'*S*)-N^2,N^4-bis(*tert*-butoxycarbonyl)-N^4-[$N^{2'}$-(9-fluorenylmethyloxycarbonyl)-2'-aminohexyl]-2,4-diaminobutanoic acid (**14**).

Similar procedures were used for synthesis of triamino acids branched with longer (C6 and C8) alkyl chains. The diamino acid **10** was treated with the chiral aldehydes **8** and **9** in presence of $NaBH_3CN$ to produce the triamino carboxylic acids **12** and **13**, respectively. Subsequent Boc protection

gave the monomers **15** and **16**, respectively (figure 4.3).

Three different strategies for the synthesis of 4-L-azalysine have been described. The first strategy involved L-serine as the starting material which was converted into methyl (*S*)-oxazolidine-4-carboxylate in three steps. In next five steps, it was converted into the end product *via* Garner's aldehyde. A second strategy involved the use of L-asparagine that was converted into *N*-protected 2,3-diaminopropionic ester, followed by reductive amination with *N*-Boc-2-aminoacetaldehyde. Strategic manipulation of protecting groups produced the final desired product in another four steps [22, 23]. The third strategy was a solid-phase dependent procedure to synthesize di- or polycationic amino acid building blocks. In this protocol, protected aziridine-2-methanol was loaded onto a trityl bromide resin, followed by ring opening with a variety of primary amines. After detachment of the product from solid support, the primary alcohol was converted into a carboxylic acid [24]. For synthesis of the triamino acids with different distances between the alpha-carbon and the secondary amine of the side chain we opted for a short route starting with the respective amino acids, ortnithine, diaminopropanoic and diaminobutanoic acid. We have reported on synthesis of a couple of these triamino acids but with a different choice of protection scheme [53, 75]. As with the branched derivative we wished to have building blocks for termination of a peptide/peptoid with possibility for extension on the side chain and therefore an Fmoc-protection on the side chain amino group and the N^2-Boc protection was used on the diamino acid.

The synthetic pathway is similar to that for the compounds with aliphatic branching except that *N*-Fmoc-glycinal (**19**) was used instead of the branched aminoaldehydes. The *N*-Fmoc-glycinal was synthesized from of the inexpensive starting material 3-aminopropane-1,2-diol (**17**) which was Fmoc protected to form **18** and then oxidatively cleaved with periodate to give **19** (figure 4.4) [79].

Reductive amination reaction with compound **19** and the respective N^{α}-Boc-diamino acids **10**, **20**, **21** in acetic acid/methanol (1:99, v/v) using $NaBH_3CN$ at room temperature resulted in the triamino acid derivatives **22–24**. After work up and purification by column chromatography Boc protection on the secondary amine was achieved by treatment with $(Boc)_2O$ to afford the products (*S*)-N^2,N^3-bis-*tert*-butoxycarbonyl-N^3-[*N*-

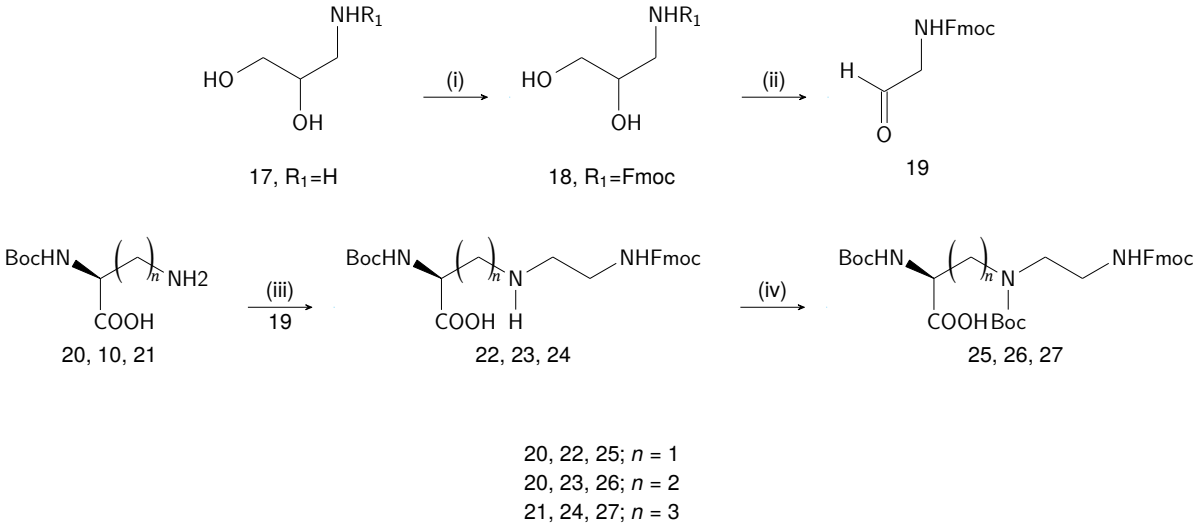

Figure 4.4: Synthesis of triamino acid building blocks with different distances between the α-amino group and the secondary amine. (i) Fmoc-OSu, MeOH/ pyridine, rt, 18 h (ii) $NaIO_4$, THF, rt, 8 h (iii) $NaBH_3CN$, 1% AcOH in methanol, rt, 18 h (iv) $(Boc)_2O$, water:dioxane (v/v, 1:1), 10% aq. Na_2CO_3, rt, 18 h.

(9-fluorenylmethyloxycarbonyl)-2-aminoethyl]-2,3-diaminopropanic acid (**25**), (*S*)-N^2,N^4-bis-*tert*-butoxycarbonyl-N^4-[*N*-(9-fluorenylmethyloxycarbonyl)-2-aminoethyl]-2,4-diaminobutanoic acid (**26**) and (*S*)-N^2,N^5-bis-*tert*-butoxycarbonyl-N^5-[*N*-(9-fluorenylmethyloxycarbonyl)-2-aminoethyl]-2,3-diaminopentanoic acid (**27**).

4.3 Conclusion

We have revealed a facile synthetic procedure for the preparation of suitably protected triamino acids in decent to good yields. Thus an extension of the available arsenal of triamino acids building blocks with varying lipophilicity and that can carry up to three positive charges is provided. Starting from *N*-Fmoc-2-alkyl amino acids (**1–3**) with varied chain length of the alkyl group, we converted them into the corresponding aminoaldehydes (**7–9**) in two steps. These aldehydes were protected and suitable for reductive amination reaction with the protected diamino acid N^{α}-Boc-L-Dab (**10**). The resulting alkyl branched triamino acids were Boc-protected to obtain the final monomers (**14–16**). In addition another series of triamino acids with different distances between the alpha-carbon and the secondary amine of the side chain (**25–27**) were made by reductive amination with *N*-Fmoc-glycinal (**19**) and a series of N^{α}-Boc diamino acids (**20**, **10**, **21**). This facile and variable procedure provided novel amino acids with hydrocarbon branching of the aminoethyl extension and convenient synthesis of triamino acids with different distances between the alpha-carbon and the secondary amine. The final monomers were suitably protected for their incorporation at the N-terminus of a peptide/peptoid sequence by Fmoc-based solid-phase synthesis while enabling further functionalization of the side chain when still attached to the support.

4.4 Experimental Section

Melting points of the compounds were recorded using Büchi Melting Point apparatus (B-545) and were uncorrected. Reactions under anhydrous conditions were carried out under a nitrogen atmosphere. Column chromatography was performed with silica gel 60 (particle size 0.040–0.063 mm, 230–400

mesh, Aldrich) and analytical grade solvents. Thin layer chromatography (TLC) was conducted on glass plates coated with silica gel 60 F_{254}, obtained from Merck. TLC plates were visualized by UV light (254 or 360 nm) and/or by staining with I_2 by keeping the plates in an iodine chamber. ^{1}H NMR (400 MHz) and ^{13}C NMR (100 MHz) spectra were recorded on a Bruker DRX-400 in $CDCl_3/CD_3OD$ at 25°C. Chemical shifts are reported in ppm relative to TMS (Me_4Si as internal standard, δ = 0 ppm) or the deuterated solvent as the internal standard for ^{1}H and ^{13}C NMR. Coupling constants ($\mathcal{J}$ values) are given in Hz. The following abbreviations are used in connection with NMR spectra: s = singlet, br s = broad singlet, d = doublet, dd = double doublet, t = triplet, q = quartet and m = multiplet. Structural assignments are based on DEPT-135, COSY and HMQC where applicable. HRMS (ESI-TOF) was recorded on a Micromass LCT either in positive ion mode or in negative ion mode. Specific rotation measurements were performed using an Autopol IV Automatic Polarimeter (Rudolph Research Analytical). RP-HPLC analysis of final building blocks is reported in [74]. THF, CH_2Cl_2, toluene, hexane, and Et_2O were dried by standard procedures and stored over molecular sieves (4 Å). *N*-(9-Fluorenylmethyloxycarbonyl)-2-aminoacetaldehyde (**19**) [79], (*S*)-*N*-(9-fluorenylmethoxycarbonyl)-2-aminohexanal (**7**) [31] and (*S*)-N^2-*tert*-butoxycarbonyl-N^5-[*N*-(9-fluorenylmethyloxycarbonyl)-2-aminoethyl]-2,5-diaminopentanoic acid (**24**) [79] were synthesized as reported (see [74]). All other solvents and chemicals were of reagent grade and used without further purification. 2-Alkyl amino acids **1**, **2** and **3** were purchased from Watanabe Chemical Industries, Ltd., Japan and Boc-protected amino acids **10**, **20** and **21** were purchased from IRIS Biotech, Germany. Other reagents were obtained from common commercial sources and used as received.

4.4.1 General procedure for synthesis of ethylthio esters (4, 5 and 6)

To a solution of Fmoc-amino acids (**1–3**, 1.3 mmol) in anhydrous dichloromethane (DCM, 20 mL) at rt, ethanethiol (5 mmol) was added dropwise, followed by addition of solid DCC (1.6 mmol) and (DMAP, 0.25 mmol) under inert atmosphere. The reaction mixture was stirred for 2 h at rt. Progress

of the reaction was monitored by TLC. Upon complete conversion of the starting material into product, water (20 mL) was added into the reaction mixture and the layers were separated. The organic layer was collected and washed with brine (2 x 10 mL), dried over Na_2SO_4 and concentrated to dryness under reduced pressure to get the crude materials. Pure products (**4–6**) were obtained by eluting the crude through a short column of silica gel.

(*S*)-S-Ethyl *N*-(9-fluorenylmethoxycarbonyl)-2-aminohexanthioate (4)

Compound **4** was purified by flash column chromatography using 0 to 25% ethyl acetate (EtOAc) in hexane as eluent to afford a white amorphous solid (0.36 g, 71%); m.p. 116–117°C. R_f = 0.54 (EtOAc/hexane, 1:5, v/v). ^{1}H NMR (400 MHz, $CDCl_3$): δ = 7.69 (d, $\mathcal{J}$ = 7.6 Hz, 2 H, Ar-H), 7.54 (t, $\mathcal{J}$ = 7.2 Hz, 2 H, Ar-H), 7.33 (t, $\mathcal{J}$ = 7.6 Hz, 2 H, Ar-H), 7.24 (t, $\mathcal{J}$ = 7.6 Hz, 2 H, Ar-H), 5.13 (d, $\mathcal{J}$ = 8.0 Hz, 1 H, NH), 4.44–4.40 (m, 1 H, NCOOCH_{2a}CH), 4.36–4.30 (m, 2 H, NCOOCH_{2b}CH, 2-CH), 4.17 (t, $\mathcal{J}$ = 6.8 Hz, 1 H, $NCOOCH_2CH$), 2.81 (q, $\mathcal{J}$ = 7.2 Hz, 2 H, $COSCH_2CH_3$), 1.85–1.80 (m, 1 H, 3-CH_{2a}), 1.57–1.51 (m, 1 H, 3-CH_{2b}), 1.30–1.23 (m, 4 H, 4-CH_2, 5-CH_2), 1.18 (t, $\mathcal{J}$ = 7.2 Hz, 3 H, $COSCH_2CH_3$), 0.83 (t, $\mathcal{J}$ = 6.8 Hz, 3 H, 6-CH_3) ppm. ^{13}C NMR (100 MHz, $CDCl_3$): δ = 201.1 (COS), 156.0 (NCOO), 144.1, 143.9, 141.5 (C-Ar), 127.9, 127.2, 125.2, 120.1 (CH-Ar), 67.2 ($NCOOCH_2CH$), 61.1 (C-2), 47.4 ($NCOOCH_2CH$), 32.8 (C-3), 27.5 (C-4), 23.4 (SCH_2CH_3), 22.4 (C-5), 14.6 (SCH_2CH_3), 14.0 (C-6) ppm. MS-ESI (*m/z*): calcd. for $C_{23}H_{28}NO_3S$ $[M+H]^+$ 398.1784; found 398.1779.

(*S*)-S-Ethyl *N*-(9-fluorenylmethoxycarbonyl)-2-aminooctanthioate (5)

Compound **5** was purified by flash column chromatography using 0 to 25% EtOAc in hexane as eluent to afford a white amorphous solid (0.33 g; 86%); m.p. 96–99°C. R_f = 0.56 (EtOAc/hexane, 1:5, v/v). ^{1}H NMR (400 MHz, $CDCl_3$): δ = 7.70 (d, $\mathcal{J}$ = 7.6 Hz, 2 H, Ar-H), 7.55 (t, $\mathcal{J}$ = 7.2 Hz, 2 H, Ar-H), 7.33 (t, $\mathcal{J}$ = 7.6 Hz, 2 H, Ar-H), 7.25 (t, $\mathcal{J}$ = 7.6 Hz, 2 H, Ar-H), 5.11 (d, $\mathcal{J}$ = 8.4 Hz, 1 H, NH), 4.44–4.40 (m, 1 H, NCOOCH_{2a}CH), 4.36–4.30 (m, 2 H, NCOOCH_{2b}CH, 2-CH), 4.17 (t, $\mathcal{J}$ = 6.8 Hz, 1 H, $NCOOCH_2CH$), 2.82 (q, $\mathcal{J}$ = 7.2 Hz, 2 H, $COSCH_2CH_3$), 1.84–1.78 (m, 1 H, 3-CH_{2a}), 1.57–1.49 (m, 1 H, 3-

CH_{2b}), 1.26–1.16 (m, 11 H, 4-CH_2, 5-CH_2, 6-CH_2, 7-CH_2, COSCH_2CH_3), 0.81 (t, J = 6.8 Hz, 3 H, 8-CH_3) ppm. ^{13}C NMR (100 MHz, $CDCl_3$): δ = 201.1 (COS), 156.0 (NCOO), 144.1, 143.9, 141.5 (C-Ar), 127.9, 127.2, 125.2, 120.1 (CH-Ar), 67.2 (NCOO*C*H_2CH), 61.1 (C-2), 47.4 (NCOOCH_2*C*H), 33.1 (C-3), 31.7 (C-4), 29.0 (C-5), 25.3 (C-6), 23.4 (S*C*H_2CH$_3$), 22.7 (C-7), 14.7 (SCH_2*C*H$_3$), 14.2 (C-8) ppm. MS-ESI (*m/z*): calcd. for $C_{25}H_{32}NO_3S$ $[M+H]^+$ 426.2103; found 426.2101.

(*S*)-S-Ethyl *N*-(9-fluorenylmethoxycarbonyl)-2-aminodecan-thioate (6)

Compound **6** was purified by flash column chromatography using 0 to 20% EtOAc in hexane as eluent to afford a white amorphous solid (0.39 g; 87%); m.p. 92–93°C. R_f = 0.59 (EtOAc/hexane, 1:5, v/v). ^{1}H NMR (400 MHz, $CDCl_3$): δ = 7.69 (d, J = 7.6 Hz, 2 H, Ar-H), 7.54 (t, J = 7.2 Hz, 2 H, Ar-H), 7.33 (t, J = 7.6 Hz, 2 H, Ar-H), 7.24 (t, J = 7.6 Hz, 2 H, Ar-H), 5.13 (d, J = 8.4 Hz, 1 H, NH), 4.44–4.39 (m, 1 H, NCOOCH_{2a}CH), 4.36–4.30 (m, 2 H, NCOOCH_{2b}CH, 2-CH), 4.17 (t, J = 6.8 Hz, 1 H, NCOOCH$_2$C*H*), 2.81 (q, J = 7.2 Hz, 2 H, COSCH_2CH$_3$), 1.84–1.77 (m, 1 H, 3-CH_{2a}), 1.56–1.50 (m, 1 H, 3-CH_{2b}), 1.26–1.16 (m, 15 H, 4-CH_2, 5-CH_2, 6-CH_2, 7-CH_2, 8-CH_2, 9-CH_2, COSCH$_2$CH_3), 0.80 (t, J = 6.8 Hz, 3 H, 10-CH_3) ppm. ^{13}C NMR (100 MHz, $CDCl_3$): δ = 201.1 (COS), 155.9 (NCOO), 144.0, 143.9, 141.5 (C-Ar), 127.9, 127.2, 125.2, 120.1 (CH-Ar), 67.2 (NCOO*C*H_2CH), 61.1 (C-2), 47.4 (NCOOCH$_2$*C*H), 33.1 (C-3), 32.0 (C-4), 29.5, 29.3, 25.4 (C-5, C-6, C-7, C-8), 23.4 (S*C*H_2CH$_3$), 22.8 (C-9), 14.6 (C-10), 14.2 (SCH_2*C*H$_3$) ppm. MS-ESI (*m/z*): calcd. for $C_{27}H_{36}NO_3S$ $[M+H]^+$ 454.2416; found 454.2413.

4.4.2 General procedure for synthesis of aliphatic amino aldehydes (7, 8 and 9)

Ethylthio esters (**4**–**6**, 0.35 mmol) were dissolved in dry acetone (6 mL) under inert atmosphere. 10% Pd/C was added to the solution followed by addition of triethylsilane (0.56 mmol) whereupon the mixture was stirred at rt. Progress of the reaction was monitored by TLC. After 2 h, the reaction was stopped by passing it through a short pad of celite and washed with acetone (3 x 6 mL). The combined organic layers was evaporated to dryness under reduced pressure and dissolved in ethylacetate (15 mL). After wash-

ing the organic layer with brine (2 x 8 mL) it was dried over Na_2SO_4 and concentrated under reduced pressure to get the crude products. Subsequent purification by silica gel column chromatography yielded compounds **7**–**9**.

(*S*)-*N*-(9-Fluorenylmethoxycarbonyl)-2-aminooctanal (8)

Compound **8** was purified by flash column chromatography using 0 to 60% EtOAc in hexane as eluent to afford a white amorphous solid (0.26 g; 92%); m.p. 75–76°C. R_f = 0.28 (EtOAc/hexane, 1:5, v/v). ^{1}H NMR (400 MHz, $CDCl_3$): δ = 9.59 (s, 1 H, CHO), 7.77 (d, $\mathcal{J}$ = 7.6 Hz, 2 H, Ar-H), 7.60 (d, $\mathcal{J}$ = 7.2 Hz, 2 H, Ar-H), 7.40 (t, $\mathcal{J}$ = 7.2 Hz, 2 H, Ar-H), 7.32 (t, $\mathcal{J}$ = 7.6 Hz, 2 H, Ar-H), 5.30 (d, $\mathcal{J}$ = 6.4 Hz, 1 H, NH), 4.43 (d, $\mathcal{J}$ = 6.8 Hz, 2 H, NCOOCH_2CH), 4.34–4.29 (m, 1 H, 2-CH), 1.94–1.89 (m, 1 H, NCOOCH$_2$C*H*), 1.66–1.58 (m, 1 H, 3-CH_{2a}), 1.33–1.26 (m, 9 H, 3-CH_{2b}, 4-CH_2, 5-CH_2, 6-CH_2, 7-CH_2), 0.87 (t, $\mathcal{J}$ = 7.2 Hz, 3 H, 8-CH_3) ppm. ^{13}C NMR (100 MHz, $CDCl_3$): δ = 199.3 (CHO), 156.3 (NCOO), 143.8, 141.4 (C-Ar), 127.7, 127.1, 125.0, 120.0 (CH-Ar), 67.0 (NCOO*C*H$_2$CH), 60.3 (C-2), 47.2 (NCOOCH$_2$*C*H), 31.5 (C-3), 29.2 (C-4), 29.0 (C-5), 25.0 (C-6), 22.5 (C-7), 14.0 (C-8) ppm. MS-ESI (*m/z*): calcd. for $C_{23}H_{28}NO_3$ $[M+H]^+$ 366.2064; found 366.2069.

(*S*)-*N*-(9-Fluorenylmethoxycarbonyl)-2-aminodecanal (9)

Compound **9** was purified by flash column chromatography using 0 to 80% EtOAc in hexane as eluent to afford a white amorphous solid (0.36 g; 84%); m.p. 69–70°C. R_f = 0.35 (EtOAc/hexane, 1:5, v/v). ^{1}H NMR (400 MHz, $CDCl_3$): δ = 9.58 (s, 1 H, CHO), 7.77 (d, $\mathcal{J}$ = 7.6 Hz, 2 H, Ar-H), 7.60 (d, $\mathcal{J}$ = 7.6 Hz, 2 H, Ar-H), 7.40 (t, $\mathcal{J}$ = 7.6 Hz, 2 H, Ar-H), 7.32 (t, $\mathcal{J}$ = 7.6 Hz, 2 H, Ar-H), 5.31 (d, $\mathcal{J}$ = 6.8 Hz, 1 H, NH), 4.43 (d, $\mathcal{J}$ = 6.8 Hz, 2 H, NCOOCH_2CH), 4.34–4.29 (m, 1 H, 2-CH), 4.23 (t, $\mathcal{J}$ = 6.8 Hz, 1 H, NCOOCH$_2$C*H*), 1.93–1.89 (m, 1 H, 3-CH_{2a}), 1.65–1.58 (m, 1 H, 3-CH_{2b}), 1.33–1.26 (m, 12 H, 4-CH_2, 5-CH_2, 6-CH_2, 7-CH_2, 8-CH_2, 9-CH_2), 0.88 (t, $\mathcal{J}$ = 7.2 Hz, 3 H, 10-CH_3) ppm. ^{13}C NMR (100 MHz, $CDCl_3$): δ = 199.3 (CHO), 156.0 (NCOO), 143.8, 143.7, 141.3 (C-Ar), 127.7, 127.1, 125.0, 120.0 (CH-Ar), 67.0 (NCOO*C*H$_2$CH), 60.3 (C-2), 47.2 (NCOOCH$_2$*C*H), 31.8, 29.3, 29.2, 25.0, 22.6 (C-3, C-4, C-5, C-6, C-7, C-8, C-9), 14.1 (C-10) ppm. MS-ESI (*m/z*): calcd. for $C_{25}H_{32}NO_3$ $[M+H]^+$ 394.2377; found 394.2390.

4.4.3 General procedure for synthesis of triamino acids 11, 12 and 13

Boc-L-Dab-OH (**10**, 0.5 mmol) was dissolved in 1% acetic acid (AcOH) in methanol (MeOH, 10 mL) and kept stirring at rt. The respective amino aldehydes (**7**–**9**, 0.46 mmol) were added into the reaction mixture slowly followed by addition of $NaBH_3CN$ (1.14 mmol). The reaction mixture was stirred at rt for 18 h. The progress of the reaction was monitored by TLC. On attaining maximum conversion, the reaction mixture was evaporated to dryness and was dissolved in ethylacetate (20 mL). Organic layer was washed with water (10 mL) and brine (10 mL x 2), dried over Na_2SO_4 and evaporated to dryness under reduced pressure to get crude compounds. Pure compounds (**11**–**13**) were obtained by purification of the crude by silica gel column chromatography (figure 4.3).

(2*S*,2'*S*)-N^2-(*tert*-Butoxycarbonyl)-N^4-[$N^{2'}$-(9-fluorenylmethyloxycarbonyl)-2'-aminohexyl]-2,4-diaminobutanoic acid (11)

Compound **11** was purified by flash column chromatography using 0 to 15% MeOH in dichloromethane containing 1% AcOH as eluent to afford a white amorphous solid (0.265 g; 50%); m.p. 93–97°C. R_f = 0.34 (MeOH/AcOH/DCM, 7.5:1:91.5, v/v/v) ^{1}H NMR (400 MHz, $CDCl_3$): δ = 7.72 (d, J = 7.2 Hz, 2 H, Ar-H), 7.59 (d, J = 7.2 Hz, 2 H, Ar-H), 7.36 (t, J = 7.2 Hz, 2 H, Ar-H), 7.27 (d, J = 7.6 Hz, 2 H, Ar-H), 5.89 (br s, 1 H, NHCOO), 5.79 (br s, 1 H, NHCOO), 4.40–4.34 (m, 1 H, 2-CH), 4.25–4.17 (m, 2 H, NCOOCH_2CH), 4.02–3.96 (m, 1 H, $NCOOCH_2CH$), 3.88–3.85 (m, 1 H, 2'-CH), 3.26–3.13 (m, 2 H, 4-CH_2) 3.03–2.93 (m, 2 H, 1'-CH_2), 2.12–2.01 (m, 3 H, 3-CH_{2a}, 3'-CH_2), 1.75–1.68 (m, 1 H, NH), 1.43–1.32 (m, 14 H, 3-CH_{2b}, 4'-CH_2, 5'-CH_2, $C(CH_3)_3$), 0.90–0.86 (m, 3 H, 6'-CH_3) ppm. ^{13}C NMR (100 MHz, $CDCl_3$): δ = 177.6 (COOH), 156.7, 155.7 (2 x NCOO), 144.1, 141.3 (C-Ar), 127.7, 127.1, 125.5, 125.4, 120.0 (CH-Ar), 79.7 ($C(CH_3)_3$), 67.1 ($NCOOCH_2CH$), 51.4 (C-2), 50.8 (C-1'), 49.6 (C-2'), 48.7 (C-4), 47.3 ($NCOOCH_2CH$), 32.2, 31.7, 31.0 (C-3, C-3', C-4'), 28.5 ($C(CH_3)_3$), 22.4 (C-5'), 14.1 (C-6') ppm. MS-ESI (*m/z*): calcd. for $C_{30}H_{40}N_3O_6$ $[M-H]^-$ 538.2923; found 538.2918.

(2*S*,2'*S*)-N^2-(*tert*-Butoxycarbonyl)-N^4-[$N^{2'}$-(9-fluorenylmethyloxycarbonyl)-2'-aminooctyl]-2,4-diaminobutanoic acid (12)

Compound **12** It was purified by flash column chromatography using 0 to 15% MeOH in dichloromethane containing 1% AcOH as eluent to afford a white amorphous solid (0.253 g; 57%); m.p. 72–76°C. R_f = 0.46 (MeOH/AcOH/DCM, 7.5:1:91.5, v/v/v) ^{1}H NMR (400 MHz, $CDCl_3$): δ = 7.73 (d, J = 6.8 Hz, 2 H, Ar-H), 7.60 (t, J = 6.0 Hz, 2 H, Ar-H), 7.36 (t, J = 6.4 Hz, 2 H, Ar-H), 7.29–7.23 (m, 2 H, Ar-H), 5.89 (br s, 1 H, NHCOO), 5.79 (br s, 1 H, NHCOO), 4.39–4.34 (m, 1 H, 2-CH), 4.22–4.15 (m, 2 H, NCOOCH_2CH), 4.03–3.86 (m, 2 H, NCOOCH$_2$C*H*, 2'-CH), 3.29–3.06 (m, 2 H, 4-CH_2), 3.00–2.91 (m, 2 H, 1'-CH_2), 2.10–1.96 (m, 3 H, 3-CH_2, 3'-CH_{2a}), 1.72–1.69 (m, 1 H, NH), 1.38–1.09 (m, 18 H, C(CH_3)$_3$, 3'-CH_{2b}, 4'-CH_2, 5'-CH_2, 6'-CH_2, 7'-CH_2), 0.91–0.78 (m, 3 H, 8'-CH_3) ppm. ^{13}C NMR (100 MHz, $CDCl_3$): δ = 177.7 (COOH), 156.7, 155.7 (2 x NCOO), 144.2, 141.4 (C-Ar), 127.7, 127.2, 125.5, 125.4, 120.0 (CH-Ar), 79.7 (*C*(CH_3)$_3$), 67.1 (NCOO*C*H$_2$CH), 53.6 (C-2), 51.4 (C-1'), 50.7 (C-2'), 48.7 (C-4), 47.2 (NCOOCH$_2$*C*H), 32.0, 31.0, 29.1 (C-3, C-3', C-4'), 28.5 (C(*C*H_3)$_3$), 26.3 (C-5'), 26.2 (C-6'), 22.7 (C-7'), 14.2 (C-8') ppm. HRMS (ESI-TOF): calcd. for $C_{32}H_{44}N_3O_6$ $[M-H]^-$ 566.3236, found 566.3226.

(2*S*,2'*S*)-N^2-(*tert*-Butyloxycarbonyl)-N^4-[$N^{2'}$-(9-fluorenylmethyloxycarbonyl)-2'-aminodecyl]-2,4-diaminobutanoic acid (13)

Compound **13** was purified by flash column chromatography using 0 to 15% MeOH in dichloromethane containing 1% AcOH as eluent to afford a white amorphous solid (0.325 g; 60%); m.p. 49–53°C. R_f = 0.29 (MeOH/AcOH/DCM, 7.5:1:91.5, v/v/v) ^{1}H NMR (400 MHz, $CDCl_3$): δ = 7.73 (d, J = 7.6 Hz, 2 H, Ar-H), 7.60 (t, J = 6.8 Hz, 2 H, Ar-H), 7.36 (t, J = 7.6 Hz, 2 H, Ar-H), 7.29–7.25 (m, 2 H, Ar-H), 5.90–5.86 (m, 1 H, NHCOO), 4.70–4.80 (m, 1 H, NHCOO), 4.35–4.31 (m, 1 H, 2-CH), 4.27–4.16 (m, 2 H, NCOOCH_2CH), 4.04–3.86 (m, 2 H, NCOOCH$_2$C*H*, 2'-CH), 3.27–3.14 (m, 2 H, 4-CH_2), 3.02–2.92 (m, 2 H, 1'-CH_2), 2.10–2.04 (m, 3 H, 3-CH_2, 3'-CH_{2a}), 1.77–1.57 (m, 1 H, 3'-CH_{2b}), 1.38–1.19 (m, 22 H, C(CH_3)$_3$, 3'-CH_{2b}, 4'-CH_2,

5'-CH_2, 6'-CH_2, 7'-CH_2, 8'-CH_2, 9'-CH_2) 0.90–0.86 (m, 3 H, 10'-CH_3) ppm. ^{13}C NMR (100 MHz, $CDCl_3$): δ = 177.6 (COOH), 156.7, 156.0 (2 x NCOO), 144.2, 144.1, 141.4 (C-Ar), 127.9, 127.8, 127.2, 125.4, 120.0 (CH-Ar), 79.9 ($C(CH_3)_3$), 67.2 (NCOOCH_2CH), 54.6 (C-2), 51.5 (C-1'), 49.6 (C-2'), 48.8 (C-4), 47.3 (NCOOCH$_2$CH), 32.0, 31.0, 30.8, 29.6, 29.4 (C-3, C-3', C-4', C-5', C-6'), 28.5 (C(CH_3)$_3$), 26.3 (C-7'), 22.8 (C-8'), 21.0 (C-9'), 14.2 (C-10') ppm. HRMS (ESI-TOF): calcd. for $C_{34}H_{48}N_3O_6$ $[M-H]^-$ 594.3549, found 594.3455.

4.4.4 General procedure for Boc protection (14, 15 and 16)

The respective triamino acids (**11**–**13**, 0.22 mmol) were dissolved in a solvent mixture of water and dioxane (1:1, v/v, 10 mL) and then stirred at 0–5°C using an ice bath. Solid Na_2CO_3 (0.45 mmol) was added into the reaction mixture, followed by addition of Boc anhydride [$(Boc)_2O$, 0.42 mmol]. The ice bath was removed after 1 hour and the reaction mixture was stirred at rt for 18 h. The progress of the reaction was monitored by TLC. After complete reaction, the temperature of the reaction mixture was set to 0–5°C and water (10 mL) was added. 1 M HCl was added into the reaction mixture dropwise to adjust the pH of the solution (to pH 3). The product was extracted with ethylacetate (15 mL x 3). The combined ethylacetate layers was washed with water (10 mL x 2) and brine (10 mL), dried over Na_2SO_4 and evaporated to dryness under reduced pressure. The crude compounds were purified by silica gel column chromatography to afford compounds **14**–**16**.

(2*S*,2'*S*)-N^2,N^4-Bis(*tert*-butoxycarbonyl)-N^4-[$N^{2'}$-(9-fluorenylmethyloxycarbonyl)-2'-amino-hexyl]-2,4-diaminobutanoic acid (14)

Compound **14** was purified by flash column chromatography using 0 to 100% EtOAc in hexane containing 1% AcOH as eluent to afford a white amorphous solid (0.245 g; 88%); m.p. 49–52°C. R_f = 0.47 (EtOAc/AcOH/hexane, 75:1.24, v/v/v) ^{1}H NMR (400 MHz, $CDCl_3$): δ = 7.75 (d, J = 7.6 Hz, 2 H, Ar-H), 7.57 (d, J = 6.8 Hz, 2 H, Ar-H), 7.38 (t, J = 7.6 Hz, 2 H, Ar-H), 7.29 (t, J = 6.8 Hz, 2 H, Ar-H), 4.50–4.32 (m, 2 H, NCOOCH_2CH), 4.25–4.15 (m, 2 H, 2-CH, NCOOCH$_2$C*H*), 3.73–3.54 (m, 3 H, 2'-CH, 1'-CH_2), 3.42–3.38 (m, 1 H, 4-CH_{2a}), 3.32–3.30 (m, 1 H, 4-CH_{2b}), 3.14–2.89 (m, 2 H, 3-CH_2), 2.12–2.00

(m, 2 H, 3'-CH_2), 1.44–1.26 (m, 22 H, 2 x $C(CH_3)_3$, 4'-CH_2, 5'-CH_2), 0.92–0.86 (m, 3 H, 6'-CH_3) ppm. ^{13}C NMR (100 MHz, $CDCl_3$): δ = 173.8 (COOH), 156.8, 156.7, 156.2 (3 x NCOO), 143.9, 141.3 (C-Ar), 127.7, 127.1, 125.2, 125.0, 120.0 (CH-Ar), 82.1, 81.1, 80.2 (2 x $C(CH_3)_3$), 66.9, 66.3, (NCOOCH_2CH), 51.2 (C-2), 50.6 (C-1'), 49.6 (C-2'), 47.3 (NCOOCH$_2$CH), 43.6, 43.1 (C-4), 33.2, 32.9, 32.0, 31.1 (C-3, C-3'), 28.4 (2 x $C(CH_3)_3$), 27.9 (C-4'), 22.6 (C-5'), 14.0 (C-6') ppm. $[\alpha]_{24}^{D}$ = −2.0 (*c* 0.1, MeOH). HRMS (ESI-TOF): calcd. for $C_{35}H_{48}N_3O_8$ $[M-H]^-$ 638.3447, found 638.3454.

(2*S*,2'*S*)-N^4-Bis(*tert*-butoxycarbonyl)-N^4-[$N^{2'}$-(9-fluorenylmethyloxycarbonyl)-2'-amino-octyl]-N^2,2,4-diaminobutanoic acid (15)

Compound **15** was purified by flash column chromatography using 0 to 100% EtOAc in hexane containing 1% AcOH as eluent to afford a colourless sticky solid (0.232 g; 88%). R_f = 0.53 (EtOAc/AcOH/hexane, 75:1.24, v/v/v) ^{1}H NMR (400 MHz, $CDCl_3$): δ = 7.75 (d, J = 7.6 Hz, 2 H, Ar-H), 7.58 (d, J = 6.8 Hz, 2 H, Ar-H), 7.38 (t, J = 7.2 Hz, 2 H, Ar-H), 7.29 (t, J = 7.2 Hz, 2 H, Ar-H), 4.50–4.35 (m, 2 H, NCOOCH_2CH), 4.22–4.11 (m, 2 H, 2-CH, NCOOCH$_2$C*H*), 3.80–3.62 (m, 3 H, 2'-CH, 1'-CH_2), 3.66–3.60 (m, 1 H, 4-CH_{2a}), 3.49–3.44 (m, 1 H, 4-CH_{2b}), 3.22–2.88 (m, 2 H, 3-CH_2), 2.09–2.02 (m, 2 H, 3'-CH_2), 1.44 (s, 18 H, 2 x $C(CH_3)_3$), 1.33–1.24 (m, 8 H, 4'-CH_2, 5'-CH_2, 6'-CH_2, 7'-CH_2), 0.92–0.84 (m, 3 H, 8'-CH_3) ppm. ^{13}C NMR (100 MHz, $CDCl_3$): δ = 173.7 (COOH), 157.0, 156.24, 156.18, 155.6 (3 x NCOO), 144.1, 141.3 (C-Ar), 127.8, 127.2, 125.3, 125.1, 120.1 (CH-Ar), 82.0, 80.9, 80.8, 80.2 (2 x $C(CH_3)_3$), 66.3, 66.1 (NCOOCH_2CH), 51.4 (C-2), 50.7 (C-1'), 47.4 (NCOOCH$_2$CH), 44.0, 43.0 (C-2', C-4), 33.5, 33.2, 31.8, 31.6, 30.5, 29.8, 29.4, 29.3 (C-3, C-3', C-4', C-5', C-6'), 28.5 (2 x $C(CH_3)_3$), 22.7 (C-7'), 14.2 (C-8') ppm. $[\alpha]_{22}^{D}$ = −2.6 (*c* 0.3, MeOH). HRMS (ESI-TOF): calcd. for $C_{37}H_{52}N_3O_8$ $[M-H]^-$ 666.3760, found 666.3755.

(2*S*,2'*S*)-N^2,N^4-Bis(*tert*-butoxycarbonyl)-N^4-[$N^{2'}$-(9-fluorenylmethyloxycarbonyl)-2'-amino-decyl]-2,4-diaminobutanoic acid (16)

Compound **16** was purified by flash column chromatography using 0 to 90% MeOH in dichloromethane containing 1% AcOH as eluent to afford a white amorphous solid (0.365 g; 79%); m.p. 44–46°C. R_f = 0.58 (EtOAc/AcOH/hexane, 75:1.24, v/v/v) ^{1}H NMR (400 MHz, $CDCl_3$): δ = 7.75 (d, $\mathcal{J}$ = 7.6 Hz, 2 H, Ar-H), 7.57 (d, $\mathcal{J}$ = 6.8 Hz, 2 H, Ar-H), 7.38 (t, $\mathcal{J}$ = 7.6 Hz, 2 H, Ar-H), 7.29 (t, $\mathcal{J}$ = 6.8 Hz, 2 H, Ar-H), 4.46–4.38 (m, 2 H, NCOOCH_2CH), 4.19–4.16 (m, 2 H, 2-CH, NCOOCH$_2$C*H*), 3.82–3.71 (m, 3 H, 2'-CH, 1'-CH_2), 3.60–3.32 (m, 2 H, 4-CH_2), 3.22–2.88 (m, 2 H, 3-CH_2), 2.10–2.00 (m, 2 H, 3'-CH_2), 1.44 (s, 18 H, 2 x C(CH_3)$_3$), 1.26 (m, 12 H, 4'-CH_2, 5'-CH_2, 6'-CH_2, 7'-CH_2, 8'-CH_2, 9'-CH_2), 0.87 (t, $\mathcal{J}$ = 6.8 Hz, 3 H, 10'-CH_3) ppm. ^{13}C NMR (100 MHz, $CDCl_3$): δ = 174.0 (COOH), 156.8, 156.7, 156.1, 155.7 (3 x NCOO), 144.0, 141.3 (C-Ar), 127.7, 127.1, 125.2, 125.0, 120.0 (CH-Ar), 81.9, 81.0, 80.2 (2 x *C*(CH_3)$_3$), 66.8, 66.1 (NCOO*C*H$_2$CH), 51.3 (C-2), 50.6, 49.6 (C-1'), 47.4 (NCOOCH$_2$*C*H), 43.9, 42.9 (C-4, C-2'), 33.4, 31.9, 30.4, 29.5, 29.3 (C-3, C-3', C-4', C-5', C-6', C-7',), 28.4 (2 x C(*C*H$_3$)$_3$), 25.8 (C-8'), 22.7 (C-9'), 14.1 (C-10') ppm. $[\alpha]_{24}^{D}$ = −4.0 (*c* 0.1, MeOH). HRMS (ESI-TOF): calcd. for $C_{39}H_{56}N_3O_8$ $[M-H]^-$ 694.4073, found 694.4063.

4.4.5 General procedure for synthesis of triamino acids 22, 23 and 24

The respective *N*-Boc-L-diamino acids (**20**, **10**, **21**, 0.5 mmol) were dissolved under stirring in anhydrous methanol (10 mL, containing 1% of AcOH). *N*-(9-Fluorenylmethoxycarbonyl)glycinal (**19**, 0.46 mmol) was added to the reaction mixture under a nitrogen atmosphere, followed by the addition of sodium cyanoborohydride (1.14 mmol). The reaction mixture was stirred at room temperature for 18 h and the progress of the reaction was monitored by TLC. The solvents were evaporated *in vacuo*, and the residue was dissolved in ethyl acetate (25 mL). The organic layer was washed with water (15 mL) and brine (2 x 15 mL), dried over Na_2SO_4, filtered and concentrated under reduced pressure. The crude products were purified by eluting them with a solution of chloroform-methanol through a short silica gel column

(figure 4.4) to yield **22**–**24** respectively.

(*S*)-N^2-*tert*-Butoxycarbonyl-N^3-[*N*-(9-fluorenylmethyloxycarbonyl)-2-aminoethyl]-2,3-diaminopropionic acid (22)

Compound **22** was purified by flash column chromatography using 0 to 15% MeOH in dichloromethane containing 1% AcOH as eluent to afford a colourless sticky solid (0.2 g; 43%). R_f = 0.14 (MeOH/AcOH/DCM, 10:1:89, v/v/v) ^{1}H NMR (400 MHz, CD_3OD): δ = 7.68 (d, $\mathcal{J}$ = 7.2 Hz, 2 H, Ar-H), 7.53 (d, $\mathcal{J}$ = 7.2 Hz, 2 H, Ar-H), 7.28 (t, $\mathcal{J}$ = 7.2 Hz, 2 H, Ar-H), 7.19 (t, $\mathcal{J}$ = 7.2 Hz, 2 H, Ar-H), 4.28 (d, $\mathcal{J}$ = 6.8 Hz, 2 H, NCOOCH_2CH), 4.09 (t, $\mathcal{J}$ = 6.8 Hz, 1 H, NCOOCH$_2$CH), 4.03 (t, $\mathcal{J}$ = 6.0 Hz, 1 H, 2-CH), 3.35–3.32 (m, 2 H, NCH$_2$CH_2NHFmoc), 3.15–3.14 (m, 2 H, 3-CH$_2$), 3.08–3.05 (m, 2 H, NCH_2CH$_2$NHFmoc), 1.32 (s, 9 H, C(CH$_3$)$_3$) ppm. ^{13}C NMR (100 MHz, CD_3OD): δ = 177.4 (COOH), 159.3, 158.0 (2 x NCOO), 145.2, 142.6 (C-Ar), 128.8, 128.1, 126.1, 120.9 (CH-Ar), 81.0 (C(CH$_3$)$_3$), 68.1 (NCOOCH$_2$CH), 52.8 (C-2), 51.0 (C-3), 49.1 (NCH$_2$CH$_2$NHFmoc), 48.5 (NCOOCH$_2$$C$H), 38.6 (NCH$_2$$CH_2$NHFmoc), 28.7 (C($CH_3$)$_3$) ppm. HRMS (ESI-TOF): calcd. for $C_{25}H_{30}N_3O_6$ $[M-H]^-$ 468.2140, found 468.2147.

(*S*)-N^2-*tert*-Butoxycarbonyl-N^4-[*N*-(9-fluorenylmethyloxycarbonyl)-2-aminoethyl]-2,4-diaminobutanoic acid (23)

Compound **23** was purified by flash column chromatography using 0 to 15% MeOH in dichloromethane containing 1% AcOH as eluent to afford a colourless sticky material (0.2 g; 42%). R_f = 0.20 (MeOH/AcOH/DCM, 10:1:89, v/v/v) ^{1}H NMR (400 MHz, CD_3OD): δ = 7.67 (d, $\mathcal{J}$ = 7.6 Hz, 2 H, Ar-H), 7.52 (d, $\mathcal{J}$ = 7.6 Hz, 2 H, Ar-H), 7.27 (t, $\mathcal{J}$ = 7.6 Hz, 2 H, Ar-H), 7.19 (t, $\mathcal{J}$ = 7.6 Hz, 2 H, Ar-H), 4.27 (d, $\mathcal{J}$ = 6.8 Hz, 2 H, NCOOCH_2CH), 4.08 (t, $\mathcal{J}$ = 6.8 Hz, 1 H, NCOOCH$_2$CH), 3.90 (t, $\mathcal{J}$ = 6.0 Hz, 1 H, 2-CH), 3.34–3.32 (m, 2 H, NCH$_2$CH_2NHFmoc), 2.98–2.97 (m, 4 H, 3-CH$_2$, NCH_2CH$_2$NHFmoc), 2.06–1.99 (m, 1 H, 4-CH$_{2a}$), 1.90–1.80 (m, 1 H, 4-CH$_{2b}$, merged with other peak), 1.32 (s, 9 H, C(CH$_3$)$_3$) ppm. ^{13}C NMR (100 MHz, CD_3OD): δ = 179.9 (COOH), 159.2, 159.0 (2 x NCOO), 145.2, 142.6 (C-Ar), 128.8, 128.1, 126.1, 120.9 (CH-Ar), 80.7 (C(CH$_3$)$_3$), 68.1 (NCOOCH$_2$CH), 54.9 (C-2), 48.9 (C-3),

48.3 (NCOOCH$_2$*C*H), 46.5 (C-4), 38.5 (N*C*H$_2$CH$_2$NHFmoc), 31.2 (NCH$_2$*C*H$_2$ NHFmoc), 28.7 (C(*C*H$_3$)$_3$) ppm. HRMS (ESI-TOF): calcd. for $C_{26}H_{32}N_3O_6$ $[M-H]^-$ 482.2297, found 482.2286.

4.4.6 General procedure for synthesis of final monomers 25, 26 and 27

The respective triamino acids (**22–24**, 0.22 mmol) were dissolved in a solvent mixture of 1, 4-dioxane and water (1:1, v/v, 10 mL) under stirring at rt. After cooling in an ice-water bath solid Na_2CO_3 (0.45 mmol) was added, followed by the addition of di-*tert*-butyl dicarbonate (0.42 mmol). The ice-water bath was removed after 1 h and the reaction mixture was stirred at room temperature for 18 h. Progress of the reaction was monitored by TLC and after complete consumption of starting material, the reaction mixture was chilled in an ice-water bath, water was added and the pH of the solution was adjusted to pH 3 by dropwise addition of 1 M HCl. The product was extracted with ethyl acetate (15 mL x 3). The organic phase was washed with water (15 mL) and brine (2 x 15 mL), dried over Na_2SO_4, filtered and concentrated to dryness under reduced pressure to get a crude product. Pure compounds (**25**–**27**) were obtained by passing them through column of silica gel and eluting with solvent gradient of EtOAc in hexane containing 1% acetic acid.

(*S*)-N^2,N^3-Bis-*tert*-butoxycarbonyl-N^3-[*N*-(9-fluorenylmethyloxycarbonyl)-2-aminoethyl]-2,3-diaminopropionic acid (25)

Compound **25** was purified by flash column chromatography using 0 to 90% EtOAc in hexane containing 1% AcOH as eluent to afford a white amorphous solid (0.084 g; 67%); m.p. 76–80°C. R_f = 0.20 (EtOAc/AcOH/hexane, 80:1:19, v/v/v) ^{1}H NMR (400 MHz, $CDCl_3$): δ = 7.67 (d, $\mathcal{J}$ = 7.2 Hz, 2 H, Ar-H), 7.51 (d, $\mathcal{J}$ = 7.2 Hz, 2 H, Ar-H), 7.31 (t, $\mathcal{J}$ = 7.2 Hz, 2 H, Ar-H), 7.21 (t, $\mathcal{J}$ = 7.2 Hz, 2 H, Ar-H), 4.45–4.30 (m, 3 H, 2-CH, NCOOC*H*$_2$CH), 4.17–4.09 (m, 1 H, NCOOCH$_2$C*H*), 3.50 (br s, 2 H, NCH$_2$C*H*$_2$NHFmoc), 3.37–3.14 (m, 4 H, 3-CH$_2$, NC*H*$_2$CH$_2$NHFmoc), 1.36 (s, 18 H, 2 x C(CH$_3$)$_3$) ppm. ^{13}C NMR (100 MHz, $CDCl_3$): δ = 173.8 (COOH), 157.1, 156.7, 156.3, 155.7 (3 x NCOO),

144.0, 141.4 (C-Ar), 127.8, 127.2, 125.2, 120.1 (CH-Ar), 81.7, 81.4, 80.5 (2 x $C(CH_3)_3$), 67.6, 67.1 (NCOOCH_2CH), 54.1, 53.0 (C-2), 50.1, 49.5, 48.6, 47.6 (C-3, NCH_2CH_2NHFmoc), 47.3 (NCOOCH$_2$CH), 40.7, 40.0 (NCH$_2CH_2$NHFmoc), 28.4 (2 x C(CH_3)$_3$) ppm. $[\alpha]_{24}^{D}$ = −11.0 (*c* 0.1, MeOH). HRMS (ESI-TOF): calcd. for $C_{30}H_{38}N_3O_8$ $[M-H]^-$ 568.2664, found 568.2670.

(*S*)-N^2,N^4-Bis-*tert*-butoxycarbonyl-N^4-[*N*-(9-fluorenylmethyloxycarbonyl)-2-aminoethyl]-2,4-diaminobutanoic acid (26)

Compound **26** was purified by flash column chromatography using 0 to 15% MeOH in dichloromethane containing 1% AcOH as eluent to afford a white amorphous solid (0.085 g; 66%); m.p. 71–76°C. R_f = 0.28 (EtOAc/AcOH/hexane, 80:1:19, v/v/v) ^{1}H NMR (400 MHz, $CDCl_3$): δ = 7.69–7.67 (d, J = 7.6 Hz, 2 H, Ar-H), 7.53 (d, J = 7.2 Hz, 2 H, Ar-H), 7.32 (td, J = 7.2, 3.6 Hz, 2 H, Ar-H), 7.22 (td, J = 7.6, 2.0 Hz, 2 H, Ar-H), 4.45–4.44 (m, 1 H, NCOOCH$_2$C*H*), 4.24–4.19 (m, 1 H, 2-CH), 4.13–4.10 (m, 2 H, NCOOCH_2CH), 3.77–3.70 (m, 1 H, 3-CH_{2a}), 3.30–3.25 (m, 3 H, NCH_{2a}CH_2NHFmoc), 2.98–2.94 (m, 1 H, NCH_{2b}CH$_2$NHFmoc), 2.87–2.83 (m, 1 H, 3-CH_{2b}), 2.04–1.94 (m, 1H, 4-CH_{2a}), 1.76–1.71 (m, 1 H, 4-CH_{2b}), 1.39–1.35 (2s, 18 H, 2 x C(CH_3)$_3$) ppm. ^{13}C NMR (100 MHz, $CDCl_3$): δ = 173.0 (COOH), 158.4, 156.9, 155.6 (3 x NCOO), 144.1, 141.4 (C-Ar), 127.8, 127.2, 125.3, 120.1 (CH-Ar), 82.8, 81.7, 80.5 (2 x $C(CH_3)_3$), 67.1, 66.9 (NCOOCH_2CH), 51.2 (C-2), 50.3 (C-3), 47.4 (NCOOCH$_2$CH), 46.3, 40.7, 34.4, 29.8 (C-4, NCH_2 CH_2NHFmoc), 28.5, 28.4 (2 x C(CH_3)$_3$) ppm. $[\alpha]_{22}^{D}$ = −2.3 (*c* 0.3, MeOH). HRMS (ESI-TOF): calcd. for $C_{31}H_{40}N_3O_8$ $[M-H]^-$ 582.2821, found 582.2816.

(*S*)-N^2,N^5-Bis-*tert*-butoxycarbonyl-N^5-[*N*-(9-fluorenylmethyloxycarbonyl)-2-aminoethyl]-2,5-diaminopentanoic acid (27)

Compound **27** was purified by flash column chromatography using 0 to 15% MeOH in dichloromethane containing 1% AcOH as eluent to afford a white sticky solid material (0.097 g; 74%). R_f = 0.17 (EtOAc/AcOH/hexane, 80:1:19, v/v/v) ^{1}H NMR (400 MHz, $CDCl_3$): δ = 7.67 (d, J = 7.6 Hz, 2 H, Ar-H), 7.45 (d, J = 7.6 Hz, 2 H, Ar-H), 7.30 (t, J = 7.6 Hz, 2 H, Ar-H), 7.21 (t, J =

7.6 Hz, 2 H, Ar-H), 4.43–4.27 (m, 3 H, NCOOCH_2CH, C-2), 4.11 (t, J = 6.8 Hz, 1 H, NCOOCH$_2$CH), 3.26–3.02 (m, 6 H, 3-CH$_2$, NCH_2CH_2NHFmoc), 1.74–1.71 (m, 1 H, 4-CH$_{2a}$), 1.56–1.51 (m, 3 H, 4-CH$_{2b}$, 5-CH$_2$), 1.36 (s, 18 H, 2 x C(CH$_3$)$_3$) ppm. ^{13}C NMR (100 MHz, CDCl$_3$): δ = 175.3 (COOH), 157.0, 156.8, 155.8 (3 x NCOO), 144.0, 141.4 (C-Ar), 127.8, 127.1, 125.2, 120.1 (CH-Ar), 80.7, 80.5, 80.2 (2 x C(CH$_3$)$_3$), 67.0, 66.8 (NHCOOCH$_2$CH), 54.4, 53.0, 47.3, 46.8 (C-2, NCH$_2$CH$_2$NHFmoc), 46.4 (NHCOOCH$_2$$C$H), 40.5, 40.1, 29.9 (C-5, NCH$_2$$CH_2$NHFmoc), 28.5 (2 x C($CH_3$)$_3$), 27.0, 24.6, 24.2 (C-3, C-4) ppm. $[\alpha]_{24}^{D}$ = +3.0 (c 0.1, MeOH). HRMS (ESI-TOF): calcd. for $C_{32}H_{42}N_3O_8$ $[M–H]^-$ 596.2977, found 596.2984.

4.5 Supporting Information

S1 Supporting Information. Experimental procedures for compounds 7, 19 and 25 as well as ^{1}H NMR and ^{13}C NMR spectra of compounds 4–9, 11–16 and 22–27; RP-HPLC chromatograms of purified compounds 14–16 and 25–27. (PDF) [74]

4.6 Acknowledgements

We gratefully acknowledge financial support from the Swedish Research Council. We also thank Prof. Göran Widmalm and Wangchuk Rabten at Stockholm University for assistance with the polarimeter.

4.7 Author contributions

Conceived and designed the experiments: JM RS. Performed the experiments: JM DH. Analyzed the data: JM DH RS. Contributed reagents/materials/analysis tools: JM DH RS. Wrote the paper: JM DH RS.

5 An Enzymatic Platform for the Synthesis of Isoprenoid Precursors

Sofia B. Rodriguez, Thomas S. Leyh

The Department of Microbiology & Immunology, The Albert Einstein College of Medicine, Bronx, New York, United States of America

E-mail: tom.leyh@einstein.yu.edu

Originally published with PLOS ONE on August 25, 2014, DOI: 10.1371/journal.pone.0105594

The isoprenoid family of compounds is estimated to contain ~65,000 unique structures including medicines, fragrances, and biofuels. Due to their structural complexity, many isoprenoids can only be obtained by extraction from natural sources, an inherently risky and costly process. Consequently, the biotechnology industry is attempting to genetically engineer microorganisms that can produce isoprenoid-based drugs and fuels on a commercial scale. Isoprenoid backbones are constructed from two, five-carbon building blocks, isopentenyl 5-pyrophosphate and dimethylallyl 5-pyrophosphate, which are end-products of either the mevalonate or non-mevalonate pathways. By linking the HMG-CoA reductase pathway (which produces mevalonate) to the mevalonate pathway, these building block can be synthesized enzymatically from acetate, ATP, NAD(P)H and CoA. Here, the enzymes in these pathways are used to produce pathway intermediates and end-products in single-pot reactions and in remarkably high yield, ~85%. A strategy for the regio-specific incorporation of isotopes into isoprenoid backbones is developed and used to synthesize a series of isotopomers of diphosphomevalonate, the immediate end-product of the mevalonate pathway. The enzymatic system is shown to be robust and ca-

pable of producing quantities of product in aqueous solutions that meet or exceed the highest levels achieved using genetically engineered organisms in high-density fermentation.

5.1 Introduction

Improved access to large numbers of pure proteins, and a rapidly increasing repertoire of well characterized enzymes, isoenzymes and mutants have substantially increased the potential to utilize *in situ* metabolic pathways, or concatenated enzymatic reactions, in the synthesis of complex natural and synthetic products. Enzymes have been honed over evolutionary time to accomplish specific catalytic tasks [2, 14]. Many are extremely efficient, regio-selective catalysts, while others exhibit broad substrate specificities that can provide flexibility in synthetic schemes. Indeed, significant efforts are underway to develop enzymes whose catalytic properties have been altered to achieve specific synthetic goals [33, 40, 111]. Enzymatic synthesis has been used to produce numerous valuable compounds [21, 51, 55, 57, 62, 66, 82, 91, 110, 116, 134] and often provides significant enhancements in yield, purity, production time and cost when compared to traditional chemical synthetic methods [59, 109]. Considerable effort is being expended to develop cell-free enzymatic systems for the production of biofuels, including dihydrogen [15] and butanol [61], biomass conversion to starch [135], and high-energy-density biobatteries [140]. While enzymatic synthesis will never replace traditional synthesis, it provides a valuable adjunct to traditional approaches particularly when the objective is to build complex natural products.

The medicinal values of isoprenoids have been documented as early as 168 BC [5, 54]. Today, we are only beginning to understand the social and commercial potential of this enormous, diverse family of natural compounds, which is estimated to contain approximately 65,000 unique structures [92]. Biotechnology companies are attempting to synthesize isopreonoid-based medicines, cosmetics [93], flavors [101], fragrances [16] and biofuels [96, 107, 137] by genetically engineering plants and bacteria to produce desired isoprenoids in commercial quantities [32, 34, 107, 131]. Recent efforts along these lines include attempts to genetically engineer organisms to produce

artemesinin (an antimalarial) at costs that will significantly expand third-world access to this drug [48, 63], and to produce isoprenoid-based fuels [96, 137].

The carbon backbones of isoprenoids are assembled from two fundamental building blocks, isopentenyl 5-pyrophosphate and dimethylallyl 5-pyrophosphate [50, 104, 121, 130]. By linking the HMG-CoA reductase pathway, which produces mevalonate, to the mevalonate pathway, these building blocks can be enzymatically assembled from acetate, ATP, NAD(P)H, and CoA (figure 5.1). Alternatively, they can be synthesized using the so-called non-mevalonate pathway [105], which is mechanistically more complex and less well defined [139]. Here, ten enzymes, including those that comprise the HMG-CoA reductase and mevalonate pathways [3, 49, 83–85, 118] are strategically employed to accomplish efficient, high-yielding (>85%) single-pot syntheses of the intermediates and endproducts of the mevalonate pathway. Labeling strategies that regio-specifically position carbon and hydrogen isotopes into the building-block backbone are developed and used to synthesize and purify isotopomers of the immediate endproduct of the mevalonate pathway, diphosphomevalonate (DPM, figure 5.2) [85]. Finally, the enzymatic system is shown to be robust and capable of producing pathway end-products in simple, aqueous solutions at levels that match or exceed the highest reported levels, which are only achieved using high-density fermentation.

5.2 Materials and Methods

5.2.1 Materials

Lactate dehydrogenase (rabbit muscle), pyruvate kinase (rabbit muscle), and inorganic pyrophosphatase (Baker's yeast) were purchased from Roche Applied Science. (*R, S*)-[$^{2}H_3$]methyl-mevalonolactone, (*R, S*)-mevalonolactone, acetyl-CoA, glutamate dehydrogenase (bovine liver), acetyl-CoA synthetase (Baker's yeast), myokinase (rabbit muscle) and lysozyme (bovine) were purchased from Sigma. Sodium acetate (^{13}C, 99%), sodium acetate (^{2}H, 99%) and D_2O (99%) were purchased from Cambridge Isotope Laboratories, Inc. All other chemical reagents were of the highest grades available.

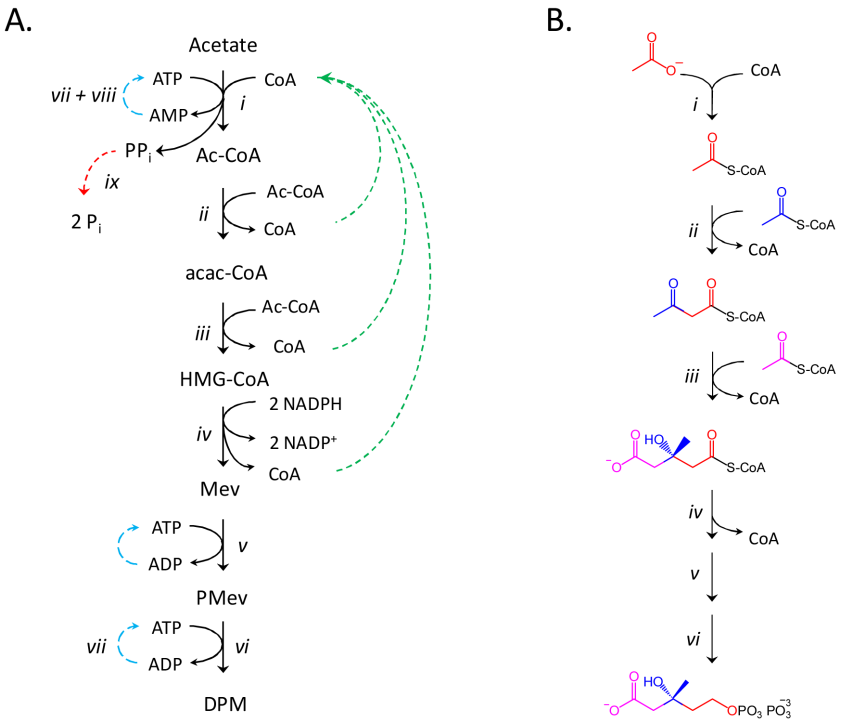

Figure 5.1: Schematics for the in-situ enzymatic synthesis of DPM and its isotopomers. **Panel A.** The enzymatic synthesis of DPM from acetate and CoA. The synthesis occurs in six steps (*i* - *vi*). CoA is consumed at reaction *i*, and regenerated at steps *ii*-*iv*. To prevent product inhibition and thermodynamically bias the system toward DPM formation, ADP (*vii*) and AMP (*vii* and *viii*) are recycled and pyrophosphate is hydrolysed (*ix*). **Panel B**. *The incorporation of acetate into DPM*. Acetate fragments are enzymatically concatenated to form the 6-carbon skeleton of DPM. Isotopic labels can be introduced at various points in the DPM synthesis to achieve a particular labeling outcome. The enyzmes used in the synthesis are as follows: *i*, acetyl-CoA synthetase; *ii*, acetoacetyl-coA thiolase; *iii*, hydroxymethylglutaryl-CoA synthase; *iv*, hydroxymethylglutaryl-CoA reductase; *v*, mevalonate kinase; *vi*, phosphomevalonate kinase; *vii*, pyruvate kinase; *viii*, adenylate kinase; *ix*, inorganic pyrophosphatase.

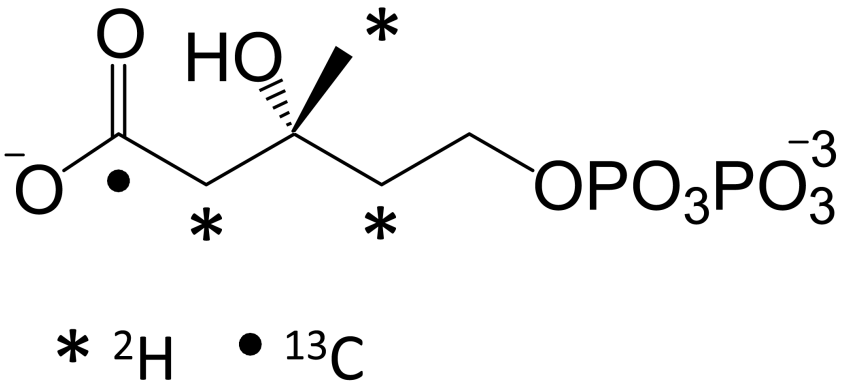

Figure 5.2: The isotopomers of (R)-diphosphomevalonate. Dots (•, [^{13}C]) and asterisks (*, [^{2}H]) mark the positions of heavy atoms in the synthesized compounds. Each mark represents a separate, singly-labeled compound. A triply-labeled compound, enriched at all of the [^{2}H]-positions, was also synthesized.

Plasmids pET28efTR (encodes a bi-functional enzyme, *Enterococcus faecalis* acetoacetyl-CoA thiolase/HMG-CoA reductase), pET28efS2 A100G (encodes *Enterococcus faecalis* HMG-CoA synthase), and pET28-efR (encodes *Enterococcus faecalis* HMG-CoA reductase) were generous provided by Prof. V. W. Rodwell [118]. Mevalonate kinase (*Staphylococcus aureus*), phosphomevalonate kinase (*Streptococcus. pneumoniae*), and diphosphomevalonate decarboxylase (*Streptococcus. pneumoniae*) were expressed and purified as described previously [3, 98].

5.2.2 Enzyme expression and purification

37°C LB/ampicillin media was inoculated with *E. coli* BL21(DE3) freshly transformed with the expression plasmid of interest. The cells were cultured to an OD_{595} of 0.8, protein expression was induced by the addition of isopropyl-1-thio-β-D-galactopyranoside (IPTG, 0.75 mM), and the incubation was continued for 4 h at 37°C. The culture temperature was then shifted to 18°C and incubation was continued for 16 h. The cells were then harvested by centrifugation (30 min, RCF 5,000 g, 4°C). The MVK [3], PMK [3] and DPM-DC (diphosphomevalonate decarboxylase) [3] expression vectors fuse a His_9-

GST-tag to the N-terminus of the enzyme; whereas, the acetoacetyl-CoA thiolase [49], HMG-CoA synthase [117] and HMG-CoA reductase [49] vectors fuse a His_6-tag to the N-terminus. Dual-tag proteins were purified using a GST resin followed by a His resin. All buffers and columns were equilibrated at 4°C prior to use. Purification began by suspending cell pellets (5.0 ml/g cell paste) in **Buffer A** [H_2KPO_4 (50 mM), NaCl (140 mM), KCl (2.7 mM), pH 7.3] supplemented with lysozyme (0.10 mg/ml), PMSF (290 µM), and pepstatin A (1.5 µM). EDTA (1.0 mM) was added to Buffer A when purifying dual-tag systems. After suspension for 1 hr at 4°C, cells were disrupted by sonication and debris was removed by centrifugation (50 min, RCF 15,000 g, 4°C). Supernatants containing dual-tag proteins were loaded onto a Glutathione Sepharose 4 FF column equilibrated with Buffer A + EDTA, the column was then washed with three column volumes of the same buffer, and protein was eluted using Tris/Cl (250 mM, pH 8.0), KCl (500 mM) and reduced glutathione (10 mM). Supernatants containing singly tagged proteins, or GST-resin eluants containing dual-tag proteins, were loaded onto a Ni-NTA column equilibrated with **Buffer B** [H_2KPO_4 (50 mM), NaCl (300 mM), imidazole (10 mM), pH 8.0]. The column was washed with **Buffer C** [H_2KPO_4 (50 mM), NaCl (300 mM), imidazole (20 mM), pH 8.0], and fusion protein was eluded with **Buffer D** [H_2KPO_4 (50 mM), NaCl (300 mM), imidazole (300 mM), β-mercaptoethanol (β-ME) (10 mM), pH 8.0]. Glycerol was then added to the singly-tagged eluants (5% v/v) and stored (see below). Tags were removed from the dual-tag proteins by incubation with PreScission protease [106] during overnight dialysis at 4°C against Hepes/K^+ (50 mM, pH 8.0) containing DTT (10 mM, dithiothreitol) and KCl (100 mM). Following proteolysis, the dialysate was passed over a GSTrap column to remove the GST-tagged protease. The purity of the single- and double-tags proteins was estimated, using SDS-PAGE, at >85 and >95%, respectively. Eluants containing purified proteins were frozen rapidly and stored at −80°C.

5.2.3 Enzymatic assays

To establish conditions for the synthesis of DPM, the activity of each enzyme was assessed under the synthesis conditions. Apparent kinetic constants were extracted from reaction progress curves [66] and were in good agreement with published values (table 5.1). *Acetyl-CoA synthetase activity* was

monitored by coupling the production of AMP to the oxidation of NADH [97]. The assay conditions were as follows: inorganic pyrophosphatase (4.0 U/ml), myokinase (4.0 U/ml), PK (4.0 U/ml), LDH (lactate dehydrogenase, 8.0 U/ml), NADH (3.0 mM, $\varepsilon_{398} = 0.136\ mM^{-1}\ cm^{-1}$), acetate (2.0 mM), CoA (2.0 mM), ATP (4.0 mM), PEP (6.0 mM), $MgCl_2$ (1.0 mM + [nucleotide]), KCl (50 mM), β-ME (10 mM). *Acac-Coa thiolase activity* was monitored by following the appearance of acac-CoA (acetoacetyl-CoA) at 302 nm [25]. The conditions were: Ac-CoA (acetyl-CoA) (6.0 mM), $MgCl_2$ (2.0 mM). *HMG-CoA synthase activity* was monitored at 386 nm ($=0.61\ mM^{-1}\ cm^{-1}$) by coupling the production of 3-hydroxy-3-methyl glutaryl-CoA to the oxidation of NADPH using HMG-CoA reductase. The conditions were: HMG-CoA reductase (1.0 μM), acac-CoA (1.0 mM), Ac-CoA (1.0 mM), NADPH (1.5 mM), KCl (50 mM), β-ME (10 mM). *HMG-CoA reductase activity* was monitored by following oxidation of NADPH. The conditions were: 3-hydroxy-3-methyl glutaryl-CoA (0.50 mM), NADPH (0.20 mM), KCl (50 mM), β-ME (10 mM). *Mevalonate kinase activity* was monitored by coupling the production of ADP to the oxidation of NADH [3, 98]. The conditions were: PK (4.0 U/ml), LDH (8.0 U/ml), NADH (200 μM, $\varepsilon_{339} = 6.22\ mM^{-1}\ cm^{-1}$), PEP (7.0 mM), mevalonate (135 μM), ATP (5.0 mM), $MgCl_2$ (1.0 mM + [nucleotide]), KCl (50 mM), β-ME (10 mM). *Phosphomevalonate kinase activity* was monitored by coupling the production of ADP to the oxidation of NADH [3, 98]. The conditions were identical to those used for mevalonate kinase except phosphomevalonate (50 μM) replaced mevalonate. *DPM Decarboxylase activity* was monitored by coupling the production of ADP to the oxidation of NADH [3, 98]. The conditions were identical to those used for mevalonate kinase except diphosphomevalonate (50 μM) replaced mevalonate. In all cases, reactions were buffered with Hepes/K^+ (50 mM), pH 8.0, and $T = 25 \pm 2°C$.

5.2.4 The synthesis of (*R*)-diphosphomevalonate

DPM was synthesized in a one-pot reaction using the following conditions: Ac-CoA synthetase (2.0 μM), acac-CoA thiolase (2.0 μM), HMG-CoA synthase (4.0 μM), HMG-CoA reductase (2.0 μM), mevalonate kinase (2.0 μM), phosphomevalonate kinase (3.0 μM), pyruvate kinase (5.0 U/mL), myokinase (2.0 U/ml), inorganic pyrophosphatase (2.0 U/ml), ATP (5.0 mM), PEP (10 mM), acetate (12 mM), CoA (5.0 mM), NADPH (10 mM), KCl (50 mM), $MgCl_2$

Table 5.1: Enzymes used in the synthesis of DPM.

[a]Enzyme	EC #	Gene	Source	Substrate	[b]K_m(mM)	[b]k_{cat}(sec^{-1})
[c]ACS	6.2.1.1	*Acs1*	*S. cerevisiae*	Acetate CoA	0.28 0.24	10
[d]ACT	2.3.1.9	*mvaE*	*E. faecalis*	Ac-CoA	0.60	2.3
[d]HMGS2	2.3.3.10	*mvaS*	*E. faecalis*	acac-CoA Ac-CoA	0.015 0.35	1.0
[d]ThRed	1.1.1.34	*mvaE*	*E. faecalis*	HMG-CoA	0.023	0.55
[d]HMGR	1.1.1.34	*mvaE*	*E. faecalis*	HMG-CoA	0.020	0.67
[d]MVK	2.7.1.36	*mvaK1*	*S. aureus*	Mevalonate	0.027	19
[d]PMK	2.7.4.2	*mvaK2*	*S. pneumoniae*	P-mev	0.0042	5.0
[c]KK	2.7.1.40	*Pkm2*	*O. cuniculus*	PEP	0.040	160
[c]MK	2.7.4.3	*Ak1*	*O. cuniculus*	AMP	[e]0.50	[e]410
[c]PP_iase	3.6.1.1	*Ppa1*	*S. cerevisiae*	PP_i	[e]0.0050	[e]260

[a]Abbreviations: ACS, acetyl-CoA synthetase; ACT, acetoacetyl-CoA thiolase; HMGS2, HMG-CoA synthase; ThRed, acetoacetyl-CoA thiolase/HMG-CoA reductase (dual-function enzyme); HMGR, HMG-CoA reductase; MVK, mevalonate kinase; PMK, phosphomevalonate kinase; PK, pyruvate kinase; MK, myokinase; PP_iase, inorganic pyrophosphatase.

[b]Standard errors are <5% in all cases (see section §5.2).

[c]Obtained from commercial sources.

[d]Expressed in *E. coli* and purified.

[e]Parameters taken from literature (MK [89, 90], PP_iase [99, 141]).

(1.0 mM + [ATP]), β-ME (10 mM), Hepes/K^+ (50 mM), pH 8.0, T=25±2°C. Reactions progress was monitored by following the oxidation of NADPH associated with the HMG-CoA reductase reaction. DPM formation was assayed by adding an aliquot the DPM-synthesis reaction into a DPM decarboxylase assay mixture (DPM-DC (0.10 μM), PK (4.0 U/ml), LDH (8.0 U/ml), NADH (200 μM), PEP (4.0 mM) ATP (2.0 mM), $MgCl_2$ (1.0 mM + [nucleotide]), KCl (50 mM), β-ME (10 mM), Hepes/K^+ (50 mM), pH 8.0, T=25±2°C) and monitoring NADH oxidation at 340 nm. The assay-reaction dilution was sufficient (330-fold dilution) to prevent the HMG-CoA reductase reaction from contributing significantly to the measurement. The reactions yielded essentially quantitative conversion of acetate to the endproduct, DPM.

5.2.5 The synthesis of labeled acetyl-coA precursors

The synthesis of regiospecifically labeled DPM requires appropriately labeled Ac-CoA. Labeled Ac-CoA precursors were synthesized using the following conditions: acetyl-CoA synthetase (2.0 μM), pyrophosphatase (2.0 U/ml), labeled acetate (4.0 mM), CoA (4.0 mM), ATP (4.0 mM), $MgCl_2$ (5.0 mM), Hepes/K^+ (50 mM), pH 8.0. The reactants were mixed gently for 10 hr at T=25±2°C. Reaction progress was monitored by assaying aliquots of the reaction for AMP synthesis using the Ac-CoA synthetase assay described above. The conversion of CoA to labeled Ac-CoA was >95%.

5.2.6 Synthesis of acac-coA

The synthesis of acac-CoA was achieved using the conditions identical to those described for the synthesis of Ac-CoA with the exception that acac-CoA thiolyase (2.0 μM) and DTNB (10 mM, 5, 5'-Dithio-bis(2-nitrobenzoic acid) were present. DNTB reacts with CoA and was used to draw the acac-thiolase reaction forward. The DTNB reaction was monitored at 412 nM [60]. Acac-CoA formation was monitored at 302 nm (*see*, 5.2.3). The reaction reached completion after approximately 17 hr, after which >98% acetyl-CoA had converted to acac-CoA. The reaction was filtered (10 kDa membrane) to remove enzymes prior to using the acac-CoA in subsequent syntheses.

5.2.7 The synthesis of [1-^{13}C]DPM or [2-$^{2}H_2$]DPM

Labeled Ac-CoA (^{13}C or ^{2}H) was prepared from CoA and labeled acetate as described above (see, 5.2.5). Labeled DPM was synthesized by adding the following reagents to the labeled Ac-CoA reaction mixture: PK (10 U/mL) (U, μmoles product formed min^{-1} at a saturating substrate), HMG-CoA synthase (4.0 μM), HMG-CoA reductase (2.0 μM), MVK (2.0 μM), PMK (1.0 μM), PEP (10 mM), NADPH (5.0 mM), unlabelled acac-CoA (2.0 mM), ATP (5.0 mM), KCl (50 mM), and β-ME (10 mM). The unlabeled acac-CoA was prepared as describe above (see, 5.2.6). The reaction was stirred gently overnight (~16 h, 25±2°C), at which point >97% of the labeled Ac-CoA had incorporated into DPM. The quantitation of DPM is described above (see, 5.2.4).

5.2.8 The synthesis of DPM from acetate at high concentration

DPM synthesis was accomplished in a one-pot reaction using the following conditions: Ac-CoA synthetase (5.0 μM), acac-CoA thiolase (7.0 μM), HMG-CoA synthase (10 μM), HMG-CoA reductase (7.0 μM), mevalonate kinase (5.0 μM), phosphomevalonate kinase (3.0 μM), pyruvate kinase (10 U/mL), myokinase (5.0 U/ml), inorganic pyrophosphatase (5.0 U/ml), ATP (100 mM), PEP (800 mM), acetate (340 mM), CoA (5.0 mM), NADPH (300 mM), $MgCl_2$ (110 mM), β-ME (10 mM), Hepes/K^+ (50 mM), pH 8.0, T = 25±2°C. Reaction progress was monitored as described above (see, 5.2.3). Under the high ionic strength conditions of this reaction, the conversion of acetate to DPM decreased to sixty-three percent.

5.2.9 The synthesis of IPP from acetate at high concentration

IPP synthesis was accomplished in a one-pot reaction using the following conditions: Ac-CoA synthetase (7.0 μM), acac-CoA thiolase (10 μM), HMG-CoA synthase (12 μM), HMG-CoA reductase (10 μM), mevalonate kinase (7.0 μM), phosphomevalonate kinase (5.0 μM), diphosphomevalonate decarboxylase (3.5 μM), pyruvate kinase (20 U/mL), myokinase (7.0 /ml), inorganic pyrophosphatase (7.0 U/ml), ATP (200 mM), PEP (800 mM), acetate (340 mM),

CoA (5.0 mM), NADPH (300 mM), $MgCl_2$ (220 mM), β-ME (10 mM), Hepes/K^+ (50 mM), pH 8.0, T=25±2°C. The conversion of acetate to IPP yields nine IPP-equivalents of pyruvate (two equivalents for each of the three Ac-CoAs required to synthesize HMG-CoA (hydroxymethylglutaryl-CoA), two for conversion of Mev to DPM and one for the decarboxylation of DPM to IPP). Pyruvate was quantitated by adding an aliquot of the IPP-synthesis reaction to a lactate dehydrogenase assay mixture: (LDH (8.0 U/ml), NADH (200 μM), KCl (50 mM), β-ME (10 mM), Hepes/K^+ (50 mM), pH 8.0, T=25±2°C). Dilution of the synthesis reaction was sufficient (>500-fold) to prevent enzymes from the reaction from contributing significantly to the pyruvate measurements. Sixty-nine percent of the acetate was converted to DPM.

5.2.10 The synthesis of DPM from (R/S)-mevalonate at high concentration

DPM synthesis was accomplished in a reaction using the following conditions: mevalonate kinase (5.0 μM), phosphomevalonate kinase (3.0 μM), pyruvate kinase (10 U/mL), (*R/S*)-mevalonate (370 mM), ATP (50 mM), PEP (350 mM), $MgCl_2$ (60 mM), β-ME (7.0 mM), Hepes/K^+ (50 mM), pH 8.0, T=25±2°C. Reaction progress was monitored as described above (see, 5.2.3). It should be noted that mevalonate kinase converts only the *R*-isomer of mevaloante to phosphomevalonate [29], and the enantiomeric composition of commercial (*R/S*)-mevalonate is 1:1 [66]; hence, a maximum of 50% of the commercial product can be converted to DPM. Seventy-one percent of the (*R*)-mevalonate in the (*R/S*)-mixture was converted to DPM.

5.2.11 The synthesis of IPP from (R/S)-mevalonate at high concentration

IPP synthesis was accomplished in a reaction using the following conditions: mevalonate kinase (5.0 μM), phosphomevalonate kinase (3.0 μM), diphosphomevalonate decarboxylase (1.6 μM), pyruvate kinase (10 U/mL), (*R/S*)-mevalonate (375 mM), ATP (50 mM), PEP (450 mM), $MgCl_2$ (60 mM), β-ME (7.0 mM), Hepes/K^+ (50 mM), pH 8.0, T=25±2°C. The conversion of (*R/S*)-mevalonate to IPP was monitored by following the formation of pyru-

vate using lactate dehydrogenase (see, 5.2.9). Seventy-seven percent of the (*R*)-mevalonate in the (*R/S*)-mixture was converted to IPP.

5.2.12 The purification (*R*)-diphosphomevalonate

To maximize the purity and recovery of DPM, PEP (which chromatographs near DPM) was converted to pyruvate by adding one PEP-equivalent of ADP to the synthesis reaction mixture. Small and large molecules were separated by ultrafilitration (10-kDa cutoff). The small-molecule filtrate was passed through a 35 mL bed of anion exchange resin (AG MP-1) equilibrated with Hepes/K^+ (10 mM, pH 7.5), and the column was "washed" with five volumes of equilibration buffer. The compounds were eluted using a 750 ml, linear salt gradient (0–1.0 M KCl) at 2.0 mL/min. DPM eluted at 0.32 mM KCl and contained <1% nucleotide. To remove excess KCl and concentrate the DPM, the purified compound was loaded onto a 5.0 ml bed of AG MP-1 equilibrated with NH_4HCO_3 (10 mM, pH 7.5). The column was then "washed" with five volumes of NH_4HCO_3 (10 mM, pH 7.5) before eluting the DPM with 1.8 volumes of NH_4HCO_3 (350 mM, pH 7.5). Excess NH_4HCO_3 was removed by rotary evaporation at 45°C. The desalted compounds were dissolved in ultra pure water (2.0 mL) and the solution was adjusted to pH 7.5 with KOH. NH_4HCO_3 in the desalted, purified DPM was measure using an enzymatic assay that couples the reduction of $NADP^+$ to the synthesis of glutamate from and α-ketoglutarate [94]. The assay conditions were as follows: α-ketoglutarate (5.0 mM), $NADP^+$ (0.20 mM), glutamate dehydrogenase (14 U/mL), Hepes/K^+ (45 mM) pH 8.0 at T=25±2°C. The /DPM stoichiometry was ~4:1. The DPM concentration and purity, presence of mevalonate and phosphomevalonate, were determined spectrophotometrically using the assay described above (see, 5.2.3), and the purified compounds were stored in Hepes/K^+ (10 mM, pH 8.0) at −80°C.

5.2.13 NMR protocols

One dimensional NMR was used to confirm the structure and isotopic labeling of the DPM isotopomers. A Bruker DRX 300 MHz spectrometer equipped with a 5 mm broadband probe was used to acquire data. Sample temperature was 25±2°C. Proton spectra were the average of 32 scans (64K points

each) acquired over 20 ppm using a 1.0 s recycle delay. The residual water signal was suppressed by presaturation of the HOD resonance. Spectra were processed with 1.0 Hz line broadening, and proton chemical shifts were referenced to 3-(trimethylsilyl) propionate [129]. Proton-decoupled carbon spectra were the average of 100 scans (61K points each) acquired over 315 ppm using a 3.0 s recycle delay. Spectra were processed with a 1.5 Hz line broadening, and chemical shifts were referenced indirectly [129]. Proton-decoupled phosphorus spectra were the average of 256 scans (64K points each) acquired over 50 ppm using a 6.0 s recycle delay. Spectra were processed with a 3.0 Hz line broadening, and chemical shifts were referenced to phosphocreatine [43].

5.3 Results and Discussion

5.3.1 The enzymatic synthesis of DPM

Diphosphomevalonate is synthesized from acetate, ATP and NADPH in six consecutive enzymatic steps (*i* - *vi*, figure 5.1). The first four reactions produce mevalonate from 3 acetate, 3 ATP, and 2 NADPH [28, 29, 100]. CoA, which acts as an acetyl-carrier, is consumed in reaction *i*, and regenerated in reactions *ii*, *iii* and *iv* (see, dashed green arrows, figure 5.1). Reactions *v* and *vi* are catalyzed by kinases that phosphorylate mevalonate to produce the pyrophosphoryl-group of DPM. To bias the reactions toward the endproduct and avoid product inhibition, ADP and AMP were recycled to ATP using pyruvate kinase and myokinase, and PP_i was hydrolyzed to P_i using inorganic pyrophosphatase. In total, nine enzymes were used in the synthesis [3, 49, 83–85, 118].

Enzymes *ii* - *vi* were cloned, expressed in *E. coli* and purified (see, 5.2); *i* and *vii* - *ix* were obtained from commercial sources. The purified enzymes were 80–95% pure, as judged by Comassie staining [87] of SDS PAGE [113] gels, and were obtained in yields of 30–40 mg pure protein/liter of *E. coli*. The kinetic constants of the purified enzymes were determined under the conditions used for the synthesis, and were in good agreement with literature values (table 5.1). The assays are described in 5.2.3 . The enzymes showed no significant loss of activity over an 8 month period when frozen

rapidly and stored at −80°C in Hepes (50 mM, pH 8.0), 150 mM KCl, 5% glycerol (v/v).

The relative enzyme concentrations used in the DPM syntheses were determined empirically by adjusting concentrations such that flux through the pathway was not rate-limited by any single step. This was accomplished by setting PMK (*vi*) at a fixed concentration and titrating each preceding enzyme successively until the DPM-synthesis rate was 80–90% of the maximum rate achievable at each step. For example, MVK (*v*) was titrated at a fixed concentration of PMK until the rate of DPM synthesis became independent of MVK concentration – the maximum rate. The MVK concentration was then adjusted to allow 80–90% of the maximum rate, and an analogous procedure was performed with HMG-CoA reductase (*iv*). The procedure was performed in succession for each enzyme in the pathway to determine the relative enzyme concentrations to be used in the synthesis. Once relative concentrations were established, the absolute concentrations were set to achieve the desired reaction times, which ranged from 8–72 hr. Mevalonate kinase from *S. aureus* was selected because, unlike the *S. pneumoniae* enzyme, it is not allosterically inhibited by DPM [66].

Substrates were set at saturating, sub-inhibiting concentrations. ATP, a substrate for five of the enzymes (*i*, *v*, *vi*, *vii* and *viii*), was set at 5.0 mM, which ranges from 5.8–68×K_m. Typical substrate concentrations of the other reactants were as follows: acetate (12 mM, 42×K_m); CoA (2.0 mM , 8.0×K_m); NADPH (10 mM, 320×K_m); and PEP (10 mM, 250×K_m). Under these conditions, and using the enzyme concentrations detailed in *Synthesis of (R)-diphosphomevalonate* (5.2), ~98% of the acetate was incorporated into DPM in this single-pot reaction.

5.3.2 The incorporation of isotopes into DPM

The regiospecific incorporation of isotopes has proven extremely valuable in the elucidation of metabolism [37, 56, 132] and determining enzyme mechanism [58]. Indeed, this was the basis for the discovery of the non-mevalonate pathway of isoprenoid biosynthesis [104]. The enzymatic scheme shown in 5.1 offers a flexible and efficient means of synthesizing numerous radiolabeled and stable isotopomers of mevalonate, many of which are not commercially available. The six-carbon backbone of DPM is constructed in

the first three enzymatic steps of the scheme (*i* – *iii*). Each step adds a single acetate to the CoA thioester R-group. The pattern of acetate incorporation into the R-group, and ultimately DPM, is shown in figure 5.1. Acetate is first esterfied onto the CoA thiol, and subsequent two-carbon units are added by forming carbon-carbon bonds with the existing R-group. Isotopes can be incorporated into specific positions in DPM (figure 5.2) using labeled acetate or acetyl-CoA, or *via* solvent exchange with exchange-sensitive intermediates. Achieving certain labeling patterns required removal of enzymes by ultrafiltration at intermediate stages of the synthesis, and/or that reactions were run in D_2O (see below).

5.3.3 The synthesis of [2, 4, 6,-$^2H_7$]- and [6-$^2H_3$]DPM

The compounds were synthesized in approximately 50 mg quantites in one-pot reactions using commercial [2-$^2H_3$]acetate or (*R, S*)-[6-$^2H_3$]mevalonolactone as starting material (see, *Supplementary Material*). Reactions were complete after 22 hrs, and virtually quantitative conversion of starting material to DPM was achieved in all cases. Approximately ~86% of the maximum theoretical maximum yield of DPM was obtained after purification (see, 5.2). The labeling of DPM was confirmed using ^1H NMR (figure S1 from [103]).

5.3.4 Synthesis of [4-$^2H_2$]DPM

The synthesis of [4-$^2H_2$]DPM was carried out in several steps. First, unlabeled Ac-CoA was synthesized using acetyl-CoA synthetase (*i*) and inorganic pyrophosphatase (*ix*) (see, *Synthesis of acetyl-CoA*, 5.2). Acetyl-CoA thiolyase (*ii*) and DTNB (in excess over Ac-CoA) were then added to form acac-CoA. DTNB reacts quantitatively with CoA [60] and was used to draw the unfavorable acac-CoA-forming reaction to completion [49]. Acac-CoA tautomerizes [17], and its enol-form exchanges protons with solvent (figure 5.3). To streamline the synthesis, both enzymatic reactions were run in D_2O. ^1H NMR confirmed that exchange was complete and occurred exclusively at the C_4-position of DPM (figure S1 from [103]). It is notable that this exchange suggests the possibility of using equilibrium isotope exchange to produce Ac-CoA in which the methyl-protons have been exchanged with solvent. To attach the third acetate without forming unlabelled acac-CoA,

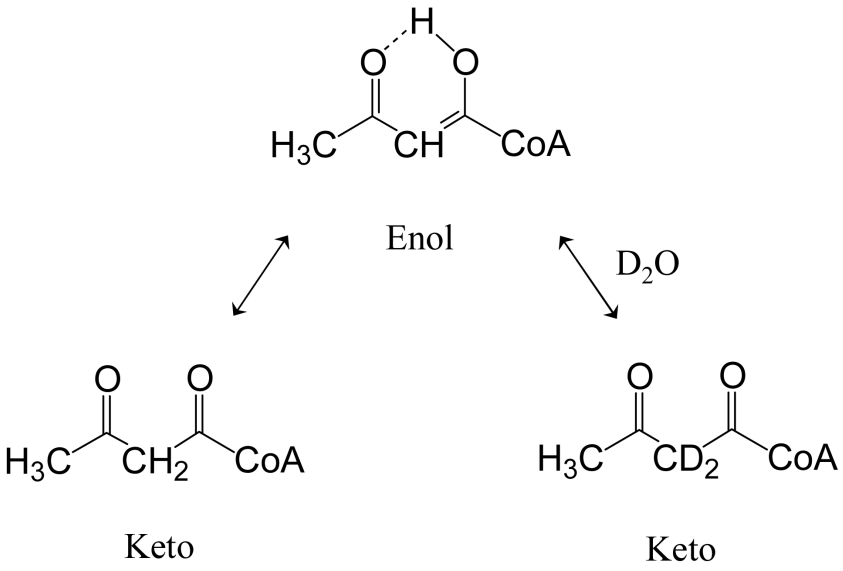

Figure 5.3: Tautomerization of acetoacetyl-CoA. Tautomerization allows H/^{2}H-exchange at the C_2-position of the 3-oxobutyryl-moiety of acac-CoA, and thus provides the precursor for the synthesis of [4-$^2H_2$]DPM.

which would dilute isotopic enrichment, the Ac-CoA thiolyase was removed by ultrafiltration before adding the reactants that complete the synthesis of DPM (see, *Synthesis of [4-$^2H_2$]-DPM, Supplementary Material*). The reactions were essentially quantitative and the production of DPM was ~96% of the theoretical maximum.

5.3.5 The synthesis of [1-^{13}C]- and [2-$^2H_2$]DPM

The strategy used to synthesize these compounds was similar to that used in the synthesis of [4-$^2H_2$]DPM. Unlabeled acac-CoA was synthesized, the enzymes used in the synthesis were "strained" from the reaction by ultrafiltration, labeled Ac-CoA was then added along with the enzymes, and reagents needed to complete the synthesis of DPM (see, 5.2). Care was taken to ensure that the Ac-CoA remaining in the acac-CoA synthesis reaction was ~0.2% of the labeled Ac-CoA used in the subsequent conversion to DPM. The yield was quantitative; DPM levels reached ~95% of the theoretical maximum.

5.3.6 Confirming the structure and labeling patterns of the compounds

The specificity and efficiency of isotopic labeling were assessed using ^{1}H and ^{13}C NMR. Deuterium incorporation at a given position was assessed by quantitating the loss of proton signal at that position. The ^{1}H NMR spectra of the synthesized compounds are compiled in figure 5.4 and figure S1 from [103]. In all cases, proton signal at the targeted position(s) was below detection (i.e., >97% incorporation efficiency) and the integrated intensities of the remaining proton peaks were identical within error (±3%); thus, deuterium did not incorporate significantly into positions other than the target sites. Comparison of the ^{1}H spectra of [1-^{13}C]- and natural abundance C_1-DPM reveals that the AB quartet associated with the C_2 of DPM (2.41 ppm) is split to into an ABX pattern by the incorporation of ^{13}C (figure 5.4). This splitting is consistent only with ^{13}C incorporation at C_1. If the synthesis had resulted in a significant fraction of natural abundance C_1-DPM, the AB and ABX resonances are expected to overlap. Close inspection of the upfield doublet of the ABX pattern gives no indication of the AB species (figure 5.4 inset) indicating that the incorporation efficiency is quite high (>95%). The labeling specificity of [1-^{13}C]DPM is given by the ^{13}C spectrum (figure 5.4), which shows the expected C_1-resonance [68] and no detectible signal at the positions associated with the other carbon atoms in the molecule (dotted arrows). The integrity of the pyrophosphoryl moiety was confirmed using ^{31}P NMR (figure S2 from [103]).

5.3.7 The synthesis of highly concentrated DPM and isopentenyldiphosphate

Given the considerable societal value of isoprenoids, the difficulties obtaining them, and the current efforts to bio-synthesize these compounds at commercial scale, it was of interest to assess the potential of the *in-situ* enzymatic synthesis to produce large quantities of product. Toward this end, the velocity of the acetate-to-DPM conversion was studied as a function of initial-reactant concentration with the goal of determining the highest, useful concentrations. The system proved remarkably robust. Only slight inhibition (~30%) was observed at 0.50 M acetate. PEP and NADPH could

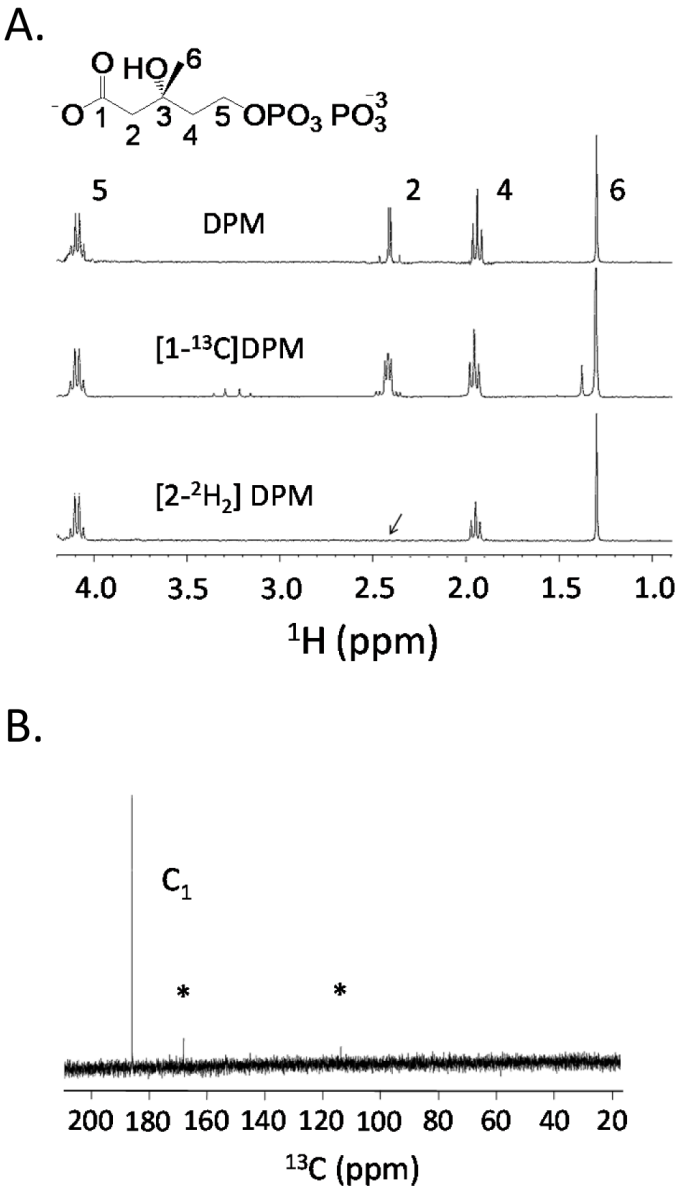

Figure 5.4: ^{1}H and ^{13}C NMR spectra of (R)-diphosphomevalonate isotopomers. Spectra indicate specificity and efficiency of labeling. **Panel A**. ^{1}H NMR spectra of labeled and unlabeled DPM. The efficiency and specificity of [$^{2}H_2$]-labeling were estimated at >98% and >95%, respectively. **Panel B**. ^{13}C NMR spectrum of [1-^{13}C]DPM. The resonance at 181 ppm corresponds to C_1. The efficiency of labeling at C_1 is estimated at >92% (see 5.3). Based on the absence of non-C_1 signals and the S/N, the labeling specificity is calculated at >98%. Asterisks indicate instrumental artifacts.

be increased to near saturation (~500 and 200 mM, respectively) without significant decrease in velocity, and ATP could be added to 0.15 M without inhibition or noticeable precipitation. The concentration-optimized system contained acetate, ATP, PEP and NADPH at 0.35, 0.10, 0.40, 0.30 M, respectively, and yielded DPM and IPP at 22 and 18 g/liter, respectively –63% and 69% conversions of acetate to product (figure 5.5). Product formation was limited by the solubility of nucleotide and high ionic strength of these reactions.. To assess whether the enzymatic system was capable of producing even higher product concentrations, DPM and IPP synthesis was initiated from mevalonate. Reactions contained (*R/S*) mevalonate, ATP, and PEP at 0.370, 0.05, 0.35 M, respectively, and yielded DPM and IPP at 42 and 35 g/liter, respectively –73% and 76% product yields (figure 5.5). The reactions conditions are further described in 5.2 (see, *Reactions that yield highly concentrated product*). 10.1371/journal.pone.0105594.g005Figure 5

The syntheses outlined in the preceding paragraph are highly scalable. Reaction yields were independent of volume from 0.10 ml–1 liter and are expected to be similar at larger volumes. Under the high ionic strength conditions of these assays, the enzymes proved to be quite stable. The majority lost ≤20% of their activity over 2 days at room temperature. The exceptions were acetoacetyl-CoA thiolyase and inorganic pyrophosphatase, which lost 63% and 72% of their activity, respectively, over this time period.

Attempts to genetically engineer plants and bacteria to produce commercial quantities of isoprenoids have met with variable success. Artemisinin, a potent antimalarial, is currently isolated from the *quinghao* plant (*Artemisia annua*) at ~3 mg/g dry weight. In contrast, genetically engineered tobacco produces artemisinin at ~0.8 mg/g dry weight [38], and transgenic yeast secrete artemisinic acid (an artemisinin precursor [11] at 100 mg/liter [102]. Using *E. coli* as the host, pathway optimization has yielded ~0.3 g/liter of artemisinic acid in shaking flasks [4, 131], high-density batch fermentation of engineered *E. coli* has produced yields as high as 23g/liter [124] and recent breakthroughs in understanding of the pathway have produced artemisinic acid at ~25 g/liter in moderately high-density *E. coli* cultures [95]. Similar efforts in *E. coli* have produce taxadiene (a precursor of Taxol, an anticancer therapeutic) at ~1g/liter in shaking flasks [1]. Production of farnesol, a relatively simple isoprenoid and potential biofuel [107], has reached 130 mg/liter in engineered *E. coli* grown in shaker flasks [126].

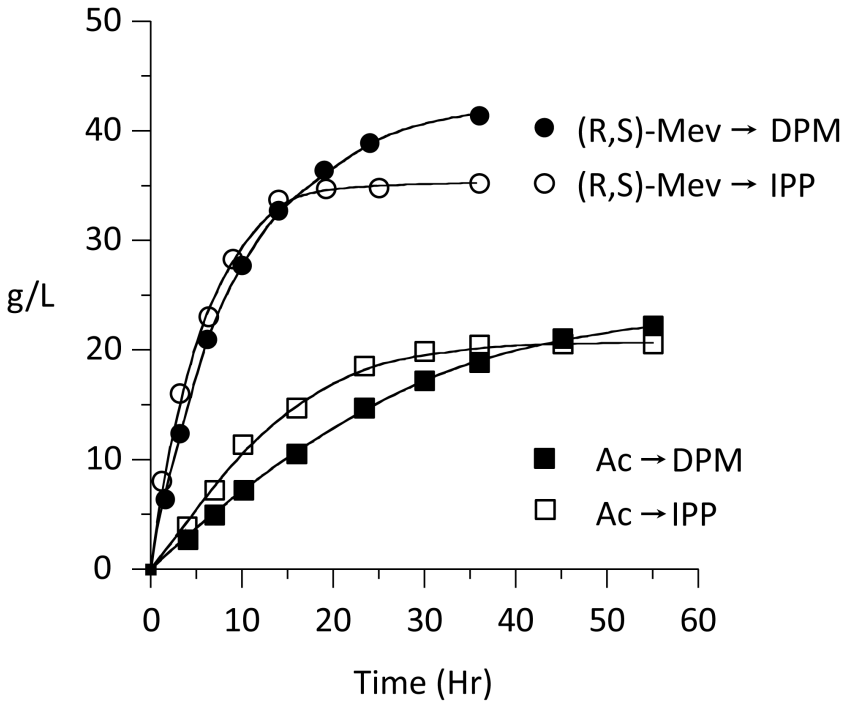

Figure 5.5: DPM and IPP synthesis at high reactant concentration. DPM and IPP were synthesized in separate, single-pot reactions. Reactions were initiated from acetate, or (R,S)-mevalonate. The conditions are described in 5.2. Reactions initiated with acetate yielded 69% conversion of acetate to IPP (○), or 63% conversion of acetate to DPM (•). Reactions starting with (R,S)-mevalonate yielded 77% conversion of (*R*)-mevalonate to IPP (□), or 73% conversion of (R)-mevalonate to DPM (■). The data points represent the average of results from three independent experiments.

While these efforts have helped define the complexities associated with expressing and controlling the isoprenoid biosynthetic pathway in living organisms, only fermentation in conjunction with genetic engineering is yielding product quantities required for successful commercial application. The cell-free approach described here yields product quantities that are comparable to, or exceed those achieved in high-density fermentation and have the advantage that product is formed in a simple aqueous system from which it can be recovered readily.

5.4 Conclusions

The enzymes that comprise the HMG CoA reductase and mevalonate pathways have been used along with enzymatic substrate-recycling and product-removal systems to efficiently synthesize intermediates and end products of these pathways in high yield. Strategies for using these enzymes to regio-specifically position isotopes in the isoprenoid backbone are described and used to synthesize and purify isotopomers of DPM, the immediate end product of the mevalonate pathway. The enzymatic platform is robust and produces isoprenoid precursors, DPM and IPP, in quantites ranging from 20–40 g/liter. These values meet or exceed all published values for isoprenoid production using genetically engineered organisms. The platform produces product in simple aqueous solutions, which, in most cases, will make isoprenoid isolation far simpler than extraction from high-density fermentums. These favorable attributes recommend the enzymatic platform as a valuable alternative to cell-culturing methods as a clean, sustainable, non-biocompetitive method for the production of isoprenoids.

5.5 Supporting Information

Figure S1 **^{1}H NMR spectra of DPM isotopomers.** The specificity and efficiency of labeling of the isotopomers were estimated based on the integration of the ^{1}H signals. The results were as follows: [4-$^{2}H_2$]DPM (96%, 95%), [6-$^{2}H_3$]DPM (97%, 95%) and [2, 4, 6-$^{2}H_7$]DPM (96%, 97%). (TIF) Figure S2 **^{31}P NMR spectrum of DPM.** The resonance positions, splitting pattern and nearly identical integrated intensities of the <- and -resonances indicate

an intact pyrophosphoryl-moiety. The asterisk identifies the resonance of phosphocreatine, which was added as an internal standard. The absence of a peak at ~5 ppm indicates that phophomevalonate is undetectable. (TIF) Text S1 (DOCX)

We thank Dr. Victor W. Rowell for providing the plasmids pET28-efTR, pET28efS2 A100G, and pET28-efR. We thank Dr. Sean Cahill for helpful discussions on the NMR data. This work was supported, in whole or in part, by National Institutes of Health Grants GM 54469, GM 106158 AI 068989.

5.6 Acknowledgements

We thank Dr. Victor W. Rowell for providing the plasmids pET28-efTR, pET28efS2 A100G, and pET28-efR. We thank Dr. Sean Cahill for helpful discussions on the NMR data. This work was supported, in whole or in part, by National Institutes of Health Grants GM 54469, GM 106158 AI 068989.

5.7 Author contributions

Conceived and designed the experiments: SBR TSL. Performed the experiments: SBR. Analyzed the data: SBR TSL. Contributed reagents/materials/analysis tools: SBR TSL. Contributed to the writing of the manuscript: SBR TSL.

Bibliography

[1] P. K. Ajikumar et al. "Isoprenoid Pathway Optimization for Taxol Precursor Overproduction in Escherichia coli". In: *Science* 330.6000 (Sept. 2010), pp. 70–74. DOI: 10.1126/science.1191652.

[2] W J Albery and J R Knowles. "Evolution of enzyme function and the development of catalytic efficiency." In: *Biochemistry* 15 (25 Dec. 1976), pp. 5631–5640. ISSN: 0006-2960.

[3] John L Andreassi, Kristina Dabovic, and Thomas S Leyh. "Streptococcus pneumoniae isoprenoid biosynthesis is downregulated by diphosphomevalonate: an antimicrobial target." In: *Biochemistry* 43 (51 Dec. 2004), pp. 16461–16466. ISSN: 0006-2960. DOI: 10.1021/bi048075t.

[4] Jennifer R. Anthony et al. "Optimization of the mevalonate-based isoprenoid biosynthetic pathway in Escherichia coli for production of the anti-malarial drug precursor amorpha-4,11-diene". In: *Metabolic Engineering* 11.1 (Jan. 2009), pp. 13–19. DOI: 10.1016/j.ymben.2008.07.007.

[5] Patrick Arsenault, Kristin Wobbe, and Pamela Weathers. "Recent Advances in Artemisinin Production Through Heterologous Expression". In: *Current Medicinal Chemistry* 15.27 (Nov. 2008), pp. 2886–2896. DOI: 10.2174/092986708786242813.

[6] Anupam Bandyopadhyay et al. "Tin(II) chloride assisted synthesis of N-protected γ-amino β-keto esters through semipinacol rearrangement." In: *Organic & biomolecular chemistry* 8 (21 Nov. 2010), pp. 4855–4860. ISSN: 1477-0539. DOI: 10.1039/c0ob00199f. URL: http://dx.doi.org/10.1039/c0ob00199f.

[7] G.K. Batchelor. *An Introduction to Fluid Dynamics*. Cambridge Mathematical Library. Cambridge University Press, 2000. ISBN: 97805216-63960. URL: https://books.google.nl/books?id=Rla7OihRvUgC.

[8] Santanu Bhattacharya and Avinash Bajaj. "Advances in gene delivery through molecular design of cationic lipids". In: *Chemical Communications* 31 (2009), pp. 4632–4656.

[9] H Blasius. "The Law of Similarity for Frictional Processes in Fluids". In: *originally in German), Forsch Arbeit Ingenieur-Wesen, Berlin* (1913), p. 131.

[10] Jon Bondebjerg et al. "A solid-phase approach to mouse melanocortin receptor agonists derived from a novel thioether cyclized peptidomimetic scaffold." In: *Journal of the American Chemical Society* 124 (37 Sept. 2002), pp. 11046–11055. ISSN: 0002-7863.

[11] Geoffrey D Brown. "The biosynthesis of artemisinin (Qinghaosu) and the phytochemistry of Artemisia annua L. (Qinghao)." In: *Molecules (Basel, Switzerland)* 15 (11 Oct. 2010), pp. 7603–7698. ISSN: 1420-3049. DOI: 10.3390/molecules15117603.

[12] Zachary Z. Brown and Christian E. Schafmeister. "Synthesis of Hexa- and Pentasubstituted Diketopiperazines from Sterically Hindered Amino Acids". In: *Organic Letters* 12.7 (Apr. 2010), pp. 1436–1439. DOI: 10.1021/ol100048g. URL: http://dx.doi.org/10.1021/ol100048g.

[13] William R Brownlie. "Re-examination of Nikuradse roughness data". In: *Journal of the Hydraulics Division* 107.1 (), pp. 115–119.

[14] Jonathan J Burbaum et al. "Evolutionary optimization of the catalytic effectiveness of an enzyme." In: *Biochemistry* 28.24 (1989), pp. 9293–9305.

[15] Julia S. Martín del Campo et al. "High-Yield Production of Dihydrogen from Xylose by Using a Synthetic Enzyme Cascade in a Cell-Free System". In: *Angewandte Chemie International Edition* 52.17 (Mar. 2013), pp. 4587–4590. DOI: 10.1002/anie.201300766.

[16] Lorenzo Caputi and Eugenio Aprea. "Use of Terpenoids as Natural Flavouring Compounds in Food Industry". In: *Recent Patents on Food, Nutrition & Agriculturee* 3.1 (Jan. 2011), pp. 9–16. DOI: 10.2174/2212798411103010009.

[17] Anna K. Cederstav and Bruce M. Novak. "Investigations into the Chemistry of Thermodynamically Unstable Species. The Direct Polymerization of Vinyl Alcohol, the Enolic Tautomer of Acetaldehyde". In: *Journal of the American Chemical Society* 116.9 (May 1994), pp. 4073–4074. DOI: 10.1021/ja00088a051.

[18] Hubert Chanson. "Hydraulics of Open Channel Flow". In: (May 25, 2004). URL: http://www.ebook.de/de/product/15272437/hubert_chanson_hydraulics_of_open_channel_flow.html.

[19] Nian-Sheng Cheng. "Formulas for Friction Factor in Transitional Regimes". In: *Journal of Hydraulic Engineering* 134.9 (Sept. 2008), pp. 1357–1362. DOI: 10.1061/(asce)0733-9429(2008)134:9(1357).

[20] Nian-Sheng Cheng and Yee-Meng Chiew. "Modified Logarithmic Law for Velocity Distribution Subjected to Upward Seepage". In: *Journal of Hydraulic Engineering* 124.12 (Dec. 1998), pp. 1235–1241. DOI: 10.1061/(asce)0733-9429(1998)124:12(1235).

[21] Qian Cheng et al. "Enzymatic total synthesis of enterocin polyketides". In: *Nature chemical biology* 3.9 (2007), p. 557.

[22] Siri Ram Chhabra, Anju Mahajan, and Weng C Chan. "Homochiral 4-azalysine building blocks: syntheses and applications in solid-phase chemistry." In: *The Journal of organic chemistry* 67 (12 June 2002), pp. 4017–4029. ISSN: 0022-3263.

[23] Siri Ram Chhabra, Anju Mahajan, and Weng C Chan. "Synthesis of novel, orthogonally protected multifunctional amino acids". In: *Tetrahedron letters* 40.26 (1999), pp. 4905–4908.

[24] Jacob Dahlqvist Clausen et al. "Solid-phase route to Fmoc-protected cationic amino acid building blocks." In: *Amino acids* 43 (4 Oct. 2012), pp. 1633–1641. ISSN: 1438-2199. DOI: 10.1007/s00726-012-1239-5.

[25] K D Clinkenbeard, T Sugiyama, and M D Lane. "Cytosolic acetoacetyl-CoA thiolase from chicken liver." In: *Methods in enzymology* 35 (1975), pp. 167–173. ISSN: 0076-6879.

[26] Stephen A. Cochrane et al. "Synthesis and StructuretextendashActivity Relationship Studies of N-Terminal Analogues of the Antimicrobial Peptide Tridecaptin A1". In: *Journal of Medicinal Chemistry* 57.3 (Feb. 2014), pp. 1127–1131. DOI: 10.1021/jm401779d. URL: http://dx.doi.org/10.1021/jm401779d.

[27] C F COLEBROOK et al. "Correspondence. Turbulent Flow in Pipes, with Particular Reference to the Transition Region between the Smooth and Rough Pipe Laws. (includes Plates)." In: *Journal of the Institution of Civil Engineers* 12.8 (Oct. 1939), pp. 393–422. DOI: 10.1680/ijoti.1939.14509.

[28] John Warcup Cornforth et al. "Substrate Stereochemistry of 3-Hydroxy-3-Methylglutaryl-Coenzyme A Synthase". In: *European Journal of Biochemistry* 42.2 (Mar. 1974), pp. 591–604. DOI: 10.1111/j.1432-1033.1974.tb03374.x.

[29] RITA H. CORNFORTH et al. "Stereospecificity of Enzymic Reactions involving Mevalonic Acid". In: *Nature* 185.4717 (Mar. 1960), pp. 923–924. DOI: 10.1038/185923a0.

[30] François Debaene et al. "Expanding the scope of PNA-encoded libraries: divergent synthesis of libraries targeting cysteine, serine and metallo-proteases as well as tyrosine phosphatases". In: *Tetrahedron* 63.28 (2007), pp. 6577–6586.

[31] François Debaene et al. "Synthesis of a PNA-encoded cysteine protease inhibitor library". In: *Tetrahedron* 60.39 (2004), pp. 8677–8690.

[32] Deepak Dugar and Gregory Stephanopoulos. "Relative potential of biosynthetic pathways for biofuels and bio-based products". In: *Nature Biotechnology* 29.12 (Dec. 2011), pp. 1074–1078. DOI: 10.1038/nbt.2055.

[33] Vincent GH Eijsink et al. "Directed evolution of enzyme stability". In: *Biomolecular engineering* 22.1 (2005), pp. 21–30.

[34] Moran Farhi et al. "Generation of the potent anti-malarial drug artemisinin in tobacco". In: *Nature Biotechnology* 29.12 (Dec. 2011), pp. 1072–1074. DOI: 10.1038/nbt.2054.

[35] Jean-Alain Fehrentz et al. "Synthesis of chiral N-protected α-amino aldehydes by reduction of N-protected N-carboxyanhydrides (UNCAs)". In: *Tetrahedron letters* 35.48 (1994), pp. 9031–9034.

[36] N W Flodin. "The metabolic roles, pharmacology, and toxicology of lysine." In: *Journal of the American College of Nutrition* 16 (1 Feb. 1997), pp. 7–21. ISSN: 0731-5724.

[37] Izabela Fokt et al. "d-Glucose and d-mannose-based metabolic probes. Part 3: Synthesis of specifically deuterated d-glucose, d-mannose, and 2-deoxy-d-glucose". In: *Carbohydrate Research* 368 (Mar. 2013), pp. 111–119. DOI: 10.1016/j.carres.2012.11.021.

[38] Jeffrey L Fox. "Interest groups jostle to influence PDUFA V". In: *Nature Biotechnology* 29.12 (Dec. 2011), pp. 1062–1062. DOI: 10.1038/nbt1211-1062.

[39] Tohru Fukuyama, Shao Cheng Lin, and Leping Li. "Facile reduction of ethyl thiol esters to aldehydes: application to a total synthesis of (+)-neothramycin A methyl ether". In: *Journal of the American Chemical Society* 112.19 (1990), pp. 7050–7051.

[40] John A Gerlt and Patricia C Babbitt. "Enzyme (re) design: lessons from natural evolution and computation". In: *Current opinion in chemical biology* 13.1 (2009), pp. 10–18.

[41] G. Gioia and Pinaki Chakraborty. "Turbulent Friction in Rough Pipes and the Energy Spectrum of the Phenomenological Theory". In: *Physical Review Letters* 96.4 (Jan. 2006). DOI: 10.1103/physrevlett.96.044502.

[42] Nigel Goldenfeld. "Roughness-Induced Critical Phenomena in a Turbulent Flow". In: *Physical Review Letters* 96.4 (Jan. 2006). DOI: 10.1103/physrevlett.96.044503.

[43] David G. Gorenstein, ed. *Phosphorous-31 NMR*. Elsevier Science, Dec. 2, 2012. 604 pp. ISBN: 0080918417. URL: http://www.ebook.de/de/product/21120952/phosphorous_31_nmr.html.

[44] R S Griffith, A L Norins, and C Kagan. "A multicentered study of lysine therapy in Herpes simplex infection." In: *Dermatologica* 156 (5 1978), pp. 257–267. ISSN: 0011-9075.

[45] D. Vaughan Griffiths and I.M. Smith. *Numerical Methods for Engineers, Second Edition.* CRC Press, 1991. ISBN: 9780849386107. URL: https://www.amazon.com/Numerical-Methods-Engineers-Vaughan-Griffiths/dp/0849386101.

[46] Ludovic Gros et al. "Evaluation of azasterols as anti-parasitics." In: *Journal of medicinal chemistry* 49 (20 Oct. 2006), pp. 6094–6103. ISSN: 0022-2623. DOI: 10.1021/jm060290f.

[47] Junke Guo. "Logarithmic matching and its applications in computational hydraulics and sediment transport". In: *Journal of Hydraulic Research* 40.5 (Sept. 2002), pp. 555–565. DOI: 10.1080/00221680209499900.

[48] Victoria Hale et al. "Microbially derived artemisinin: a biotechnology solution to the global problem of access to affordable antimalarial drugs." In: *The American journal of tropical medicine and hygiene* 77 (6 Suppl Dec. 2007), pp. 198–202. ISSN: 0002-9637.

[49] M. Hedl et al. "Enterococcus faecalis Acetoacetyl-Coenzyme A Thiolase/3-Hydroxy-3-Methylglutaryl-Coenzyme A Reductase, a Dual-Function Protein of Isopentenyl Diphosphate Biosynthesis". In: *Journal of Bacteriology* 184.8 (Apr. 2002), pp. 2116–2122. DOI: 10.1128/jb.184.8.2116-2122.2002.

[50] A. Hemmerlin et al. "Enzymes Encoded by the Farnesyl Diphosphate Synthase Gene Family in the Big Sagebrush Artemisia tridentata ssp. spiciformis". In: *Journal of Biological Chemistry* 278.34 (June 2003), pp. 32132–32140. DOI: 10.1074/jbc.m213045200.

[51] Robert HH van den Heuvel et al. "Enzymatic synthesis of vanillin". In: *Journal of agricultural and food chemistry* 49.6 (2001), pp. 2954–2958.

[52] Pak T Ho and Kheh Yong Ngu. "An effective synthesis of N-(9-fluorenylmethyloxycarbonyl). alpha.-amino aldehydes from S-benzyl thioesters". In: *The Journal of Organic Chemistry* 58.8 (1993), pp. 2313–2316.

[53] Dmytro Honcharenko et al. "Synthesis and evaluation of antineurotoxicity properties of an amyloid-upbeta peptide targeting ligand containing a triamino acid". In: *Organic and Biomolecular Chemistry* 12.34 (June 2014), pp. 6684–6693. DOI: 10.1039/c4ob00959b. URL: http://dx.doi.org/10.1039/c4ob00959b.

[54] Elisabeth Hsu. "The history of qing hao in the Chinese materia medica." In: *Transactions of the Royal Society of Tropical Medicine and Hygiene* 100 (6 June 2006), pp. 505–508. ISSN: 0035-9203. DOI: 10.1016/j.trstmh.2005.09.020.

[55] Kuo-Ting Huang et al. "Multi-enzyme one-pot strategy for the synthesis of sialyl Lewis X-containing PSGL-1 glycopeptide". In: *Carbohydrate research* 341.12 (2006), pp. 2151–2155.

[56] Yun-Qing Huang et al. "Use of isotope mass probes for metabolic analysis of the jasmonate biosynthetic pathway". In: *The Analyst* 136.7 (2011), p. 1515. DOI: 10.1039/c0an00736f.

[57] Yasuhiro Kajiwara et al. "Genetically Engineered Synthesis and Structural Characterization of Cobalt- Precorrin 5A and- 5B, Two New Intermediates on the Anaerobic Pathway to Vitamin B12: Definition of the Roles of the CbiF and CbiG Enzymes". In: *Journal of the American Chemical Society* 128.30 (2006), pp. 9971–9978.

[58] Judith P. Klinman. "The power of integrating kinetic isotope effects into the formalism of the Michaelis-Menten equation". In: *FEBS Journal* 281.2 (Sept. 2013), pp. 489–497. DOI: 10.1111/febs.12477.

[59] Kathryn M Koeller and Chi-Huey Wong. "Enzymes for chemical synthesis". In: *Nature* 409.6817 (2001), pp. 232–240.

[60] N M Kredich and G M Tomkins. "The enzymic synthesis of L-cysteine in Escherichia coli and Salmonella typhimurium." In: *The Journal of biological chemistry* 241 (21 Nov. 1966), pp. 4955–4965. ISSN: 0021-9258.

[61] Borimas Krutsakorn et al. "In vitro production of n-butanol from glucose". In: *Metabolic Engineering* 20 (Nov. 2013), pp. 84–91. DOI: 10.1016/j.ymben.2013.09.006.

[62] Balagurunathan Kuberan et al. "Enzymatic synthesis of antithrombin III–binding heparan sulfate pentasaccharide". In: *Nature biotechnology* 21.11 (2003), pp. 1343–1346.

[63] Catherine Lacaze et al. "The initial pharmaceutical development of an artesunate/amodiaquine oral formulation for the treatment of malaria: a public-private partnership". In: *Malaria Journal* 10.1 (2011), p. 142. DOI: 10.1186/1475-2875-10-142.

[64] Graham R Lawton and Daniel H Appella. "Nonionic side chains modulate the affinity and specificity of binding between functionalized polyamines and structured RNA." In: *Journal of the American Chemical Society* 126 (40 Oct. 2004), pp. 12762–12763. ISSN: 0002-7863. DOI: 10.1021/ja046436m.

[65] Jeong Tae Lee et al. "Design, syntheses, and evaluation of Taspase1 inhibitors." In: *Bioorganic & medicinal chemistry letters* 19 (17 Sept. 2009), pp. 5086–5090. ISSN: 1464-3405. DOI: 10.1016/j.bmcl.2009.07.045. URL: http://dx.doi.org/10.1016/j.bmcl.2009.07.045.

[66] Scott T Lefurgy et al. "Probing ligand-binding pockets of the mevalonate pathway enzymes from Streptococcus pneumoniae". In: *Journal of Biological Chemistry* 285.27 (2010), pp. 20654–20663.

[67] T J Lehmann and J W Engels. "Synthesis and properties of bile acid phosphoramidites 5′-tethered to antisense oligodeoxynucleotides against HCV." In: *Bioorganic & medicinal chemistry* 9 (7 July 2001), pp. 1827–1835. ISSN: 0968-0896.

[68] G. C. Levy and G. L. Nelson. *Carbon-13 nuclear magnetic resonance for organic chemists*. New York [etc.]: Wiley-Interscience, 1972.

[69] Shuolin Li and Wenxin Huai. "United Formula for the Friction Factor in the Turbulent Region of Pipe Flow". In: *PLOS ONE* 11.5 (May 2016). Ed. by Iman Borazjani, e0154408. DOI: 10.1371/journal.pone.0154408.

[70] Aleksandra Liberska et al. "Solid-phase synthesis of arginine-based double-tailed cationic lipopeptides: potent nucleic acid carriers". In: *Chemical Communications* 47.48 (2011), p. 12774. DOI: 10.1039/c1cc15805h. URL: http://dx.doi.org/10.1039/c1cc15805h.

[71] Phillip M. Ligrani and Robert J. Moffat. "Structure of transitionally rough and fully rough turbulent boundary layers". In: *Journal of Fluid Mechanics* 162.-1 (Jan. 1986), p. 69. DOI: 10.1017/s0022112086001933.

[72] Xiangli Liu, Bernard Testa, and Alfred Fahr. "Lipophilicity and Its Relationship with Passive Drug Permeation". In: *Pharmaceutical Research* 28.5 (Oct. 2010), pp. 962–977. DOI: 10.1007/s11095-010-0303-7. URL: http://dx.doi.org/10.1007/s11095-010-0303-7.

[73] C MacKellar et al. "Synthesis and physical properties of anti-HIV antisense oligonucleotides bearing terminal lipophilic groups." In: *Nucleic acids research* 20 (13 July 1992), pp. 3411–3417. ISSN: 0305-1048.

[74] Jyotirmoy Maity, Dmytro Honcharenko, and Roger Strömberg. "Electronic Supplementary Information to Synthesis of Triamino Acid Building Blocks with Different Lipophilicities". In: *PLOS ONE* 10.4 (Apr. 2015). Ed. by Stephan Neil Witt, e0124046. DOI: 10.1371/journal.pone.0124046.s001.

[75] Jyotirmoy Maity and Roger Stromberg. "N2-tert-Butoxycarbonyl-N5-[N-(9-fluorenylmethyloxycarbonyl)-2-aminoethyl]-(S)-2, 5-diaminopentanoic acid". In: *Molbank* 2014.3 (2014), p. M833.

[76] Pijus K Mandal et al. "Structure-affinity relationships of glutamine mimics incorporated into phosphopeptides targeted to the SH2 domain of signal transducer and activator of transcription 3." In: *Journal of medicinal chemistry* 52 (19 Oct. 2009), pp. 6126–6141. ISSN: 1520-4804. DOI: 10.1021/jm901105k. URL: http://dx.doi.org/10.1021/jm901105k.

[77] Milan Marek. "On the mechanism of some antimetabolic action on the biosynthesis of the "cooling protein" by pupae Galleria mellonella". In: *Comparative Biochemistry and Physiology* 35.3 (1970), pp. 737–743.

[78] Riccardo Mariani et al. "Antibiotics GE23077, novel inhibitors of bacterial RNA polymerase. Part 3: Chemical derivatization." In: *Bioorganic & medicinal chemistry letters* 15 (16 Aug. 2005), pp. 3748–3752. ISSN: 0960-894X. DOI: 10.1016/j.bmcl.2005.05.060.

[79] Nobuaki Matsumori, Rie Masuda, and Michio Murata. "Amphotericin B covalent dimers bearing a tartarate linkage." In: *Chemistry & biodiversity* 1 (2 Feb. 2004), pp. 346–352. ISSN: 1612-1880. DOI: 10.1002/cbdv.200490030.

[80] T J MCCORD, D E COOK, and L G SMITH. "THE SYNTHESIS AND BIOLOGICAL ACTIVITIES OF SOME AZA ANALOGS OF AMINO ACIDS. II. 4-AZALYSINE, AN INHIBITORY ANALOG OF LYSINE." In: *Archives of biochemistry and biophysics* 105 (May 1964), pp. 349–351. ISSN: 0003-9861.

[81] Mohammad Mehrafarin and Nima Pourtolami. "Intermittency and rough-pipe turbulence". In: *Physical Review E* 77.5 (May 2008). DOI: 10.1103/physreve.77.055304.

[82] Jonathan S Melnick et al. "An efficient enzymatic synthesis of thiamin pyrophosphate". In: *Bioorganic & medicinal chemistry letters* 13.22 (2003), pp. 4139–4141.

[83] B. Middleton. "The kinetic mechanism and properties of the cytoplasmic acetoacetyl-coenzyme A thiolase from rat liver". In: *Biochemical Journal* 139.1 (Apr. 1974), pp. 109–121. DOI: 10.1042/bj1390109.

[84] H M Miziorko and M D Lane. "3-Hydroxy-3-methylgutaryl-CoA synthase. Participation of acetyl-S-enzyme and enzyme-S-hydroxymethylgutaryl-SCoA intermediates in the reaction." In: *The Journal of biological chemistry* 252 (4 Feb. 1977), pp. 1414–1420. ISSN: 0021-9258.

[85] Henry M Miziorko. "Enzymes of the mevalonate pathway of isoprenoid biosynthesis." In: *Archives of biochemistry and biophysics* 505 (2 Jan. 2011), pp. 131–143. ISSN: 1096-0384. DOI: 10.1016/j.abb.2010.09.028.

[86] Bernhard Neises and Wolfgang Steglich. "Simple method for the esterification of carboxylic acids". In: *Angewandte Chemie International Edition in English* 17.7 (1978), pp. 522–524.

[87] Volker Neuhoff, Reinhard Stamm, and Hansjörg Eibl. "Clear background and highly sensitive protein staining with Coomassie Blue dyes in polyacrylamide gels: A systematic analysis". In: *Electrophoresis* 6.9 (1985), pp. 427–448. DOI: 10.1002/elps.1150060905.

[88] Johann Nikuradse. "Laws of flow in rough pipes". In: (1950).

[89] L NODA. "Adenosine triphosphate-adenosine monophosphate transphosphorylase. III. Kinetic studies." In: *The Journal of biological chemistry* 232 (1 May 1958), pp. 237–250. ISSN: 0021-9258.

[90] L. Noda. "The Enzymes". In: ed. by Paul D. Boyer. Elsevier Science, Oct. 28, 1970. Chap. Nucleoside triphosphate-nucleoside monophosphokinases, pp. 139–149. ISBN: 9780080865799. URL: http://www.ebook.de/de/product/15193986/unknown_author_enzymes.html.

[91] Kohji Ohdan et al. "Phosphorylase coupling as a tool to convert cellobiose into amylose". In: *Journal of biotechnology* 127.3 (2007), pp. 496–502.

[92] Eric Oldfield and Fu-Yang Lin. "Terpene Biosynthesis: Modularity Rules". In: *Angewandte Chemie International Edition* 51.5 (Nov. 2011), pp. 1124–1137. DOI: 10.1002/anie.201103110.

[93] Anne Osbourn, Rebecca J. M. Goss, and Robert A. Field. "The saponins – polar isoprenoids with important and diverse biological activities". In: *Natural Product Reports* 28.7 (2011), p. 1261. DOI: 10.1039/c1np00015b.

[94] Nazmi Özer. "A new enzyme-coupled spectrophotometric method for the determination of arginase activity". In: *Biochemical Medicine* 33.3 (June 1985), pp. 367–371. DOI: 10.1016/0006-2944(85)90012-2.

[95] C. J. Paddon et al. "High-level semi-synthetic production of the potent antimalarial artemisinin". In: *Nature* 496.7446 (Apr. 2013), pp. 528–532. DOI: 10.1038/nature12051.

[96] Pamela P. Peralta-Yahya et al. "Identification and microbial production of a terpene-based advanced biofuel". In: *Nature Communications* 2 (Sept. 2011), p. 483. DOI: 10.1038/ncomms1494.

[97] D. E. Pilloff and T. S. Leyh. "Allosteric and Catalytic Functions of the PPi-binding Motif in the ATP Sulfurylase-GTPase System". In: *Journal of Biological Chemistry* 278.50 (Sept. 2003), pp. 50435–50441. DOI: 10.1074/jbc.m306897200.

[98] D. Pilloff et al. "The Kinetic Mechanism of Phosphomevalonate Kinase". In: *Journal of Biological Chemistry* 278.7 (Nov. 2002), pp. 4510–4515. DOI: 10.1074/jbc.m210551200.

[99] Pekka Pohjanjoki et al. "Evolutionary Conservation of Enzymatic Catalysis: Quantitative Comparison of the Effects of Mutation of Aligned Residues in Saccharomyces cerevisiae and Escherichia coli Inorganic Pyrophosphatases on Enzymatic Activity †". In: *Biochemistry* 37.7 (Feb. 1998), pp. 1754–1761. DOI: 10.1021/bi971771r.

[100] G. Popják. "The Enzymes". In: ed. by Paul D. Boyer. Elsevier Science, Oct. 28, 1970. Chap. Stereospecificity of Enzymic Reactions, pp. 115–215. ISBN: 9780080865799. URL: http://www.ebook.de/de/product/15193986/unknown_author_enzymes.html.

[101] Munish Puri, Deepika Sharma, and Ashok K. Tiwari. "Downstream processing of stevioside and its potential applications". In: *Biotechnology Advances* 29.6 (Nov. 2011), pp. 781–791. DOI: 10.1016/j.biotechadv.2011.06.006.

[102] Dae-Kyun Ro et al. "Production of the antimalarial drug precursor artemisinic acid in engineered yeast." In: *Nature* 440 (7086 Apr. 2006), pp. 940–943. ISSN: 1476-4687. DOI: 10.1038/nature04640.

[103] Sofia B. Rodriguez and Thomas S. Leyh. "An Enzymatic Platform for the Synthesis of Isoprenoid Precursors". In: *PLoS ONE* 9.8 (Aug. 2014). Ed. by Y-H Percival Zhang, e105594. DOI: 10.1371/journal.pone.0105594.

[104] Michel Rohmer and Michel Rohmer. "The discovery of a mevalonate-independent pathway for isoprenoid biosynthesis in bacteria, algae and higher plants†". In: *Natural Product Reports* 16.5 (1999), pp. 565–574. DOI: 10.1039/a709175c.

[105] M Rohmer et al. "Isoprenoid biosynthesis in bacteria: a novel pathway for the early steps leading to isopentenyl diphosphate". In: *Biochemical Journal* 295.2 (Oct. 1993), pp. 517–524. DOI: 10.1042/bj2950517.

[106] Michael J. Romanowski, Jeffrey B. Bonanno, and Stephen K. Burley. "Crystal structure of the Streptococcus pneumoniae phosphomevalonate kinase, a member of the GHMP kinase superfamily". In: *Proteins: Structure, Function, and Genetics* 47.4 (June 2002), pp. 568–571. DOI: 10.1002/prot.10118.abs.

[107] Mathew A Rude and Andreas Schirmer. "New microbial fuels: a biotech perspective". In: *Current Opinion in Microbiology* 12.3 (June 2009), pp. 274–281. DOI: 10.1016/j.mib.2009.04.004.

[108] Yalin M. S. and Da Silva A. M. A. F. *Fluvial processes*. IAHR, Delft, The Netherlands, 2001.

[109] A Schmid et al. "Industrial biocatalysis today and tomorrow". In: *Nature* 409.6817 (2001), pp. 258–268.

[110] Heather L Schultheisz et al. "Pathway engineered enzymatic de novo purine nucleotide synthesis". In: *ACS chemical biology* 3.8 (2008), pp. 499–511.

[111] Shampa Sen, V Venkata Dasu, and Bisnupada Mandal. "Developments in directed evolution for improving enzyme functions". In: *Applied biochemistry and biotechnology* 143.3 (2007), pp. 212–223.

[112] I.H. Shames. *Mechanics of fluids*. McGraw-Hill series in mechanical engineering. McGraw-Hill, 1962. URL: https://books.google.nl/books?id=E5VRAAAAMAAJ.

[113] Arnold L. Shapiro, Eladio Viñuela, and Jacob V. Maizel. "Molecular weight estimation of polypeptide chains by electrophoresis in SDS-polyacrylamide gels". In: *Biochemical and Biophysical Research Communications* 28.5 (Sept. 1967), pp. 815–820. DOI: 10.1016/0006-291x(67)90391-9.

[114] Miro Smriga and Kunio Torii. "L-Lysine acts like a partial serotonin receptor 4 antagonist and inhibits serotonin-mediated intestinal pathologies and anxiety in rats." In: *Proceedings of the National Academy of Sciences of the United States of America* 100 (26 Dec. 2003), pp. 15370–15375. ISSN: 0027-8424. DOI: 10.1073/pnas.2436556100.

[115] A Strickler. "Contributions to the question of a velocity formula and roughness data for streams, channels and closed pipelines". In: (1981).

[116] Masakazu Sugiyama et al. "D-Fructose-6-phosphate aldolase-catalyzed one-pot synthesis of iminocyclitols". In: *Journal of the American Chemical Society* 129.47 (2007), pp. 14811–14817.

[117] A. Sutherlin et al. "Enterococcus faecalis 3-Hydroxy-3-Methylglutaryl Coenzyme A Synthase, an Enzyme of Isopentenyl Diphosphate Biosynthesis". In: *Journal of Bacteriology* 184.15 (Aug. 2002), pp. 4065–4070. DOI: 10.1128/jb.184.15.4065-4070.2002.

[118] Autumn Sutherlin and Victor W. Rodwell. "Multienzyme mevalonate pathway bioreactor". In: *Biotechnology and Bioengineering* 87.4 (2004), pp. 546–551. DOI: 10.1002/bit.20157.

[119] Jianjun Tao. "Critical Instability and Friction Scaling of Fluid Flows through Pipes with Rough Inner Surfaces". In: *Physical Review Letters* 103.26 (Dec. 2009). DOI: 10.1103/physrevlett.103.264502.

[120] Tullia Tedeschi et al. "A Fmoc-based submonomeric strategy for the solid phase synthesis of optically pure chiral PNAs". In: *Tetrahedron Letters* 49.33 (2008), pp. 4958–4961.

[121] Hirekodathakallu V. Thulasiram, Hans K. Erickson, and C. Dale Poulter. "A Common Mechanism for Branching, Cyclopropanation, and Cyclobutanation Reactions in the Isoprenoid Biosynthetic Path-

way". In: *Journal of the American Chemical Society* 130.6 (Feb. 2008), pp. 1966–1971. DOI: 10.1021/ja0771282.

[122] Hidetoshi Tokuyama et al. "Reduction of ethanethiol esters to aldehydes". In: *Synthesis* 2002.08 (2002), pp. 1121–1123.

[123] Rama P Tripathi et al. "Recent development on catalytic reductive amination and applications". In: *Current Organic Chemistry* 12.13 (2008), pp. 1093–1115.

[124] Hiroko Tsuruta et al. "High-Level Production of Amorpha-4,11-Diene, a Precursor of the Antimalarial Agent Artemisinin, in Escherichia coli". In: *PLoS ONE* 4.2 (Feb. 2009). Ed. by Aric Gregson, e4489. DOI: 10.1371/journal.pone.0004489.

[125] Li W. and Xu X. *Hydraulics*. Wuhan University of Hydraulic and Electrical Engineering Publishing Company Press, 2000.

[126] Chonglong Wang et al. "Farnesol production from Escherichia coli by harnessing the exogenous mevalonate pathway". In: *Biotechnology and Bioengineering* 107.3 (June 2010), pp. 421–429. DOI: 10.1002/bit.22831.

[127] Gang Wang et al. "Solid-phase synthesis of peptide vinyl sulfones as potential inhibitors and activity-based probes of cysteine proteases." In: *Organic letters* 5 (5 Mar. 2003), pp. 737–740. ISSN: 1523-7060. DOI: 10.1021/ol0275567.

[128] James J Wen and Craig M Crews. "Synthesis of 9-fluorenylmethoxycarbonyl-protected amino aldehydes". In: *Tetrahedron: Asymmetry* 9.11 (1998), pp. 1855–1858.

[129] DavidS. Wishart et al. "1H, 13C and 15N chemical shift referencing in biomolecular NMR". In: *Journal of Biomolecular NMR* 6.2 (Sept. 1995), pp. 135–140. DOI: 10.1007/bf00211777.

[130] J. Wouters et al. "Catalytic Mechanism of Escherichia coli Isopentenyl Diphosphate Isomerase Involves Cys-67, Glu-116, and Tyr-104 as Suggested by Crystal Structures of Complexes with Transition State Analogues and Irreversible Inhibitors". In: *Journal of Biological Chemistry* 278.14 (Jan. 2003), pp. 11903–11908. DOI: 10.1074/jbc.m212823200.

[131] Tao Wu et al. "[Biosynthesis of amorpha-4,11-diene, a precursor of the antimalarial agent artemisinin, in Escherichia coli through introducing mevalonate pathway]." In: *Sheng wu gong cheng xue bao = Chinese journal of biotechnology* 27 (7 July 2011), pp. 1040–1048. ISSN: 1000-3061.

[132] Yongsheng Xiao, Lei Guo, and Yinsheng Wang. "Isotope-Coded ATP Probe for Quantitative Affinity Profiling of ATP-Binding Proteins". In: *Analytical Chemistry* 85.15 (Aug. 2013), pp. 7478–7486. DOI: 10.1021/ac401415z.

[133] Xiao-Ding Xu et al. "Controlled peptide coated nanostructures via the self-assembly of functional peptide building blocks". In: *Polymer Chemistry* 3.9 (2012), pp. 2479–2486.

[134] Shigenori Yamaguchi, Hidenobu Komeda, and Yasuhisa Asano. "New enzymatic method of chiral amino acid synthesis by dynamic kinetic resolution of amino acid amides: use of stereoselective amino acid amidases in the presence of α-amino-ε-caprolactam racemase". In: *Applied and environmental microbiology* 73.16 (2007), pp. 5370–5373.

[135] C. You et al. "Enzymatic transformation of nonfood biomass to starch". In: *Proceedings of the National Academy of Sciences* 110.18 (Apr. 2013), pp. 7182–7187. DOI: 10.1073/pnas.1302420110.

[136] Zeng Yuhong and Huai Wenxin. "Application of artificial neural network to predict the friction factor of open channel flow". In: *Communications in Nonlinear Science and Numerical Simulation* 14.5 (May 2009), pp. 2373–2378. DOI: 10.1016/j.cnsns.2008.06.020.

[137] Fuzhong Zhang, Sarah Rodriguez, and Jay D Keasling. "Metabolic engineering of microbial pathways for advanced biofuels production". In: *Current Opinion in Biotechnology* 22.6 (Dec. 2011), pp. 775–783. DOI: 10.1016/j.copbio.2011.04.024.

[138] Lijuan Zhang and Robin Carmichael. *Short antimicrobial lipopeptides*. US Patent 9,278,994. Mar. 2016.

[139] Lishan Zhao et al. "Methylerythritol phosphate pathway of isoprenoid biosynthesis." In: *Annual review of biochemistry* 82 (2013), pp. 497–530. ISSN: 1545-4509. DOI: 10.1146/annurev-biochem-052010-100934.

[140] Zhiguang Zhu et al. "A high-energy-density sugar biobattery based on a synthetic enzymatic pathway". In: *Nature Communications* 5 (Jan. 2014), p. 3026. DOI: 10.1038/ncomms4026.

[141] Anton B. ZYRYANOV et al. "Mechanism by which metal cofactors control substrate specificity in pyrophosphatase". In: *Biochemical Journal* 367.3 (Nov. 2002), pp. 901–906. DOI: 10.1042/bj20020880.